

(1)

AD-A210 707

TGAL-88-06

**ITERATIVE NETWORK MAGNITUDE ESTIMATION
AND UNCERTAINTY ASSESSMENT WITH NOISY
AND CLIPPED DATA**

R.-S. Jih and R. H. Shumway

Teledyne Geotech Alexandria Laboratories
314 Montgomery Street
Alexandria, Virginia 22314-1581

Division of Statistics
University of California
Davis, CA 95616

JUNE 1988

FINAL REPORT (PART 4): TASKS 1 and 2
ARPA ORDER NO: A5143
PROJECT TITLE: Yield Estimation and Regional Location
CONTRACT: MDA903-87-C-0069

DTIC
ELECTE
AUG 01 1989
S **D**

Approved for Public Release; Distribution Unlimited

Prepared for:
DEFENSE ADVANCED RESEARCH PROJECTS AGENCY
1400 Wilson Boulevard
Arlington, VA 22209

Monitored by:
Defense Supply Service, Washington
Room 1D 245, The Pentagon
Washington, D.C. 20310

The views and conclusions contained in this report are those of the authors and should not be interpreted as representing the official policies, either expressed or implied, of the Defense Advanced Research Projects Agency or the U.S. Government.

REPORT DOCUMENTATION PAGE

1a REPORT SECURITY CLASSIFICATION Unclassified		1b RESTRICTIVE MARKINGS	
2a SECURITY CLASSIFICATION AUTHORITY		3 DISTRIBUTION/AVAILABILITY OF REPORT Approved for Public Release; Distribution Unlimited	
2b DECLASSIFICATION/DOWNGRADING SCHEDULE		5 MONITORING ORGANIZATION REPORT NUMBER(S)	
4 PERFORMING ORGANIZATION REPORT NUMBER(S) TCAL-88-06		7a NAME OF MONITORING ORGANIZATION Defense Supply Service - Washington	
6a NAME OF PERFORMING ORGANIZATION Teledyne Geotech and University of California	6b OFFICE SYMBOL (if applicable)	7b ADDRESS (City, State, and ZIP Code) Room 1D245, The Pentagon Washington, DC 20310	
6c ADDRESS (City, State, and ZIP Code) 314 Montgomery Street Alexandria, VA 22314		9 PROCUREMENT INSTRUMENT IDENTIFICATION NUMBER MDA093-87-C-0069	
8a NAME OF FUNDING / SPONSORING ORGANIZATION DARPA	8b OFFICE SYMBOL (if applicable) NMRO	10. SOURCE OF FUNDING NUMBERS	
8c ADDRESS (City, State, and ZIP Code) 1400 Wilson Boulevard Arlington, VA 22209		PROGRAM ELEMENT NO	PROJECT NO
11 TITLE (Include Security Classification) ITERATIVE NETWORK MAGNITUDE ESTIMATION AND UNCERTAINTY ASSESSMENT WITH NOISY AND CLIPPED DATA		TASK NO	WORK UNIT ACCESSION NO
12 PERSONAL AUTHOR(S) R.S. Jih and R.H. Shumway			
13a. TYPE OF REPORT Final Technical	13b TIME COVERED FROM June 87 TO June 89	14. DATE OF REPORT (Year, Month, Day) June 88	15 PAGE COUNT 65
16 SUPPLEMENTARY NOTATION			
17 COSATI CODES		18 SUBJECT TERMS (Continue on reverse if necessary and identify by block number)	
FIELD	GROUP	Magnitude estimation, censored data, iterative least squares, maximum likelihood, EM algorithm, bootstrap	
19 ABSTRACT (Continue on reverse if necessary and identify by block number)			
<p>We briefly discuss the similarities and differences between two iterative estimators that are suitable for the network m_p estimation problem, namely a modification of the Iterative Least-Squares method (ILS) due to Schmee and Hahn (1979) and the Maximum-Likelihood Estimator (MLE). Both methods reduce to the usual Least Squares Multiple Factors (LSMF) method when the censored data are deleted from the network observational data. For the censored case, the standard deviation (σ) of the obscuring noise must be solved through iteration along with the event magnitudes and the station corrections. An extra constraint on σ is necessary to determine which optimal estimation scheme is of interest. The final value of σ for each iterative scheme can be used as a good approximation to the unbiased estimate of the standard deviation of the perturbing noise. By scaling this σ value by the square root of the</p>			
20 DISTRIBUTION/AVAILABILITY OF ABSTRACT <input checked="" type="checkbox"/> UNCLASSIFIED/UNLIMITED <input type="checkbox"/> SAME AS RPT <input type="checkbox"/> DTIC USERS		21 ABSTRACT SECURITY CLASSIFICATION	
22a NAME OF RESPONSIBLE INDIVIDUAL Dr. Robert R. Blandford		22b TELEPHONE (Include Area Code) (202) 697-6523	22c OFFICE SYMBOL nmro

(19. Continued)

number of observations associated with each unknown parameter, the uncertainty in each estimated parameter can be approximated efficiently. These error estimates seem to differ from the unbiased standard errors only by a common multiplying constant across all stations and all event m_b 's.

The bootstrap method is reviewed and adapted to the case of multivariate estimation with doubly censored data. The Monte Carlo resampling is carried out among the collection of residuals instead of the observational data. The pool of residuals is enlarged to include all censored residuals for random drawing. The bootstrap result confirms the aforementioned scaling relationship between the individual error estimates and the global σ of the perturbing noise. As a result, the bootstrap/jackknife technique may not justify the considerable computational effort required for this specific application.

Accession For	
NTIS CRA&I	<input checked="" type="checkbox"/>
DTIC TAB	<input type="checkbox"/>
Unannounced	<input type="checkbox"/>
Justification	
By _____	
Distribution/	
Availability Codes	
Dist	Avail and/or Special
A-1	



SUMMARY

We briefly discuss the similarities and differences between two iterative estimators that are suitable for the network m_b estimation problem, namely a modification of the Iterative Least-Squares method (ILS) due to Schmee and Hahn (1979) and the Maximum-Likelihood Estimator (MLE). Both methods reduce to the usual Least Squares Multiple Factors (LSMF) method when the censored data are deleted from the network observational data. For the censored case, the standard deviation (σ) of the obscuring noise must be solved through iteration along with the event magnitudes and the station corrections. An extra constraint on σ is necessary to determine which optimal estimation scheme is of interest. The final value of σ for each iterative scheme can be used as a good approximation to the unbiased estimate of the standard deviation of the perturbing noise. By scaling this σ value by the square root of the number of observations associated with each unknown parameter, the uncertainty in each estimated parameter can be approximated efficiently. These error estimates seem to differ from the unbiased standard errors only by a common multiplying constant across all stations and all event m_b 's.

The bootstrap method is reviewed and adapted to the case of multivariate estimation with doubly censored data. The Monte Carlo resampling is carried out among the collection of residuals instead of the observational data. The pool of residuals is enlarged to include all censored residuals for random drawing. The bootstrap result confirms the aforementioned scaling relationship between the individual error estimates and the global σ of the perturbing noise. As a result, the bootstrap/jackknife technique

may not justify the considerable computational effort required for this specific application.

TABLE OF CONTENTS

	Page
SUMMARY	iii
TABLE OF CONTENTS	v
LIST OF FIGURES	vi
LIST OF TABLES	ix
1. INTRODUCTION	1
2. MODEL ASSUMPTIONS AND GENERAL IDEAS	3
3. ITERATIVE LEAST SQUARES METHOD	8
4. MAXIMUM-LIKELIHOOD METHOD	10
5. BOOTSTRAP METHOD	17
6. DISCUSSION AND CONCLUSIONS	37
7. ACKNOWLEDGEMENTS	39
8. REFERENCES	40
DISTRIBUTION LISTS	45

LIST OF FIGURES

Figure No.	Caption	Page
1	The log-likelihood and the squared penalty loss as a function of σ in the range from 0.10 to 1.00. The log-likelihood function attains its maximum at RMS $\sigma = 0.324$, or $\hat{\sigma}_{MLE} = 0.329$ after the D.O.F. adjustment. The squared penalty loss function $\Delta(\sigma)$ increases almost linearly as σ increases, and it has no apparent critical point in the range considered. Conceptually censored paths cannot provide more information than the non-censored paths, and therefore the $\Delta = (n_0+n_1+n_2) \sigma^2$ determines the smallest acceptable σ , which yields RMS $\sigma = 0.258$, or $\hat{\sigma}_{ILS} = 0.263$ after the D.O.F.-adjustment. Thus ILS is indeed optimal in terms of the squared penalty loss.	22
2a	The $\hat{m}_{b_{MLE}}$ and $\hat{m}_{b_{ILS}}$ versus $\hat{m}_{b_{LSMF}}$ for 110 explosions (328 phases). There is only a narrow magnitude range from about 5.7 to 6.5 in which the censoring effects of clipping or non-detection do not lead to serious bias. Compared to MLE, ILS tends to underestimate somewhat the censoring effects.	24
2b	The $\hat{m}_{b_{MLE}}$ versus $\hat{m}_{b_{ILS}}$ for 110 explosions (328 phases). Compared to MLE, ILS tends to underestimate somewhat the censoring effects.	25
3a	The receiver effects of 127 WWSSN stations indicate that ILS tends to underestimate the censoring effects due to clippings or non-detections, same as in Figures 2a and 2b.	26
3b	Comparison of the receiver effects estimated by MLE and ILS.	27
3c	Histogram of the receiver effects with bin width 0.1 unit. Circles, "+" signs, and triangles represents the spread of the 127 receiver terms estimated with LSMF, MLE, and ILS methods respectively.	28

- 4a The uncertainty estimated by ILS versus that by ILS and bootstrap. The abscissa $\text{Error}_{\text{ILS}}$ is *predicted* in an analytical manner by dividing the $\hat{\sigma}_{\text{ILS}}$ by the square root of number of associated observations. The ILS plus bootstrap method computes the ordinate with statistics from 600 Monte Carlo simulations. The highly linear relationship between these two methods strongly indicates that ILS alone would give a fairly good estimate of the uncertainty, except for the constant bias-correcting factor, 1.450. 29
- 4b Same as Figure 4a except that MLE is used instead of ILS. The magnifying factor required in this case is 1.218. 30
- 5a The $\log_{10}\sqrt{\# \text{ of observations}}$ (including signals, noises, and clips) versus the $\log_{10}(\text{uncertainty estimate})$. Filled circles represent the results from 600 bootstrap iterations. The nearly linear relationship ($X + Y \approx \log_{10}(0.381)$) indicates that the product of the $\sqrt{\# \text{ of observations}}$ and the individual error estimate will be a stable estimator of the true σ of the obscuring perturbations. The lower curve ($X + Y \approx \log_{10}(0.263)$) gives the predicted uncertainty with $\hat{\sigma}_{\text{ILS}}$. There exists a constant offset between the predicted curve and the experimental curve, which can be used to test any analytical bias-correction scheme to be developed. 31
- 5b Same as Figure 5a except that MLE is used instead of ILS. The linear relationship is as obvious as in the ILS case. The offset between the theoretical curve and the bootstrap's result is smaller, which suggests that $\hat{\sigma}_{\text{ILS}}$ requires more complicated bias corrections in addition to the D.O.F.-adjustment. The upper line ($X + Y \approx \log_{10}(0.401)$) and the lower line ($X + Y \approx \log_{10}(0.329)$) will merge together in the non-censoring case. 32
- 6a The histogram of the ILS residuals with bin width 0.1 unit. Circles, "+" signs, and triangles represents the spread of 7547 "regular residuals", 5012 "noisy residuals", and 950 "clipped residuals", respectively. The ILS residuals are slightly more concentrated than that of MLE, because $\hat{\sigma}_{\text{ILS}}$ is smaller than $\hat{\sigma}_{\text{MLE}}$. The interpolated shape of the histogram empirically justifies the idealized assumption that residuals follow a normal distribution. 34

- 6b The interpolated histogram of the MLE residuals (See Figure 6a for caption). 35
- 6c The "refined" histogram showing the effect of incorporating the censored information. Here we replaced each censored residual by its "refined" form, which is defined as the discrepancy between the final conditional expectation of the censored observation and the regressed mean. The interpolated histograms illustrate again that the Gaussian assumption is adequate. 36

LIST OF TABLES

Table No.	Title	Page
1	Epicenters and Dates	12
2	Original Data at 71 WWSSN Sites And Their Effects	13
3	Comparison of LSMF, MLE, and ILS	15
4	Comparison of MLE and MLE+Bootstrap	19
5	Comparison of ILS and ILS+Bootstrap	20

(THIS PAGE INTENTIONALLY LEFT BLANK)

1. INTRODUCTION

The problem of estimating body-wave magnitudes (m_b) using amplitudes read at a number of recording stations is frequently complicated by the fact that the data may be heavily censored. This arises either because of clipping, where all amplitudes can be determined only to exceed a given lower bound (*i.e.* the right-censored case in statistical terms), or because the signals are weaker than the ambient noise level and hence are not detected (*i.e.* the left-censored case). If one simply averages the amplitudes for those stations which detect an event, without regard for those that clipped or did not record, serious biases may result in the magnitude estimated.

The problem of jointly estimating event magnitude and station corrections (Douglas, 1966; von Seggern, 1973) using data that are incomplete because of missing station readings and censoring (above by clipping and below by noise) has been considered in Blandford and Shumway (1982). In the case where the errors in observing the amplitudes are uncorrelated from event to event and from station to station, the Expectation Maximization (EM) algorithm (Dempster *et al.*, 1977) can be used to solve the multiparametric version of the maximum likelihood estimation problems originally considered by Ringdal (1976) for the left-censored case and by von Seggern and Rivers (1978) for the doubly censored case.

We will examine the similarities and differences between two iterative estimators for censored model, namely the Iterative Least-Squares method (ILS) due to Schmee and Hahn (1979) and the Maximum-Likelihood Estimator (MLE). These two methods reduce to the same Least Squares Multiple Factors (LSMF) (Douglas, 1966) method when the censored data are deleted from the network observational data. Each method is completely characterized by

a constraint on the choice of the standard deviation (σ) of the obscuring noise, and σ is solved through iteration along with the event magnitudes and the station corrections. The final value of σ for each iterative scheme can be used as a good approximation to the unbiased estimate of the standard deviation of the perturbing noise. By scaling this σ value by the square root of the number of observations associated with each unknown parameter, the uncertainty in each estimated parameter can be approximated efficiently. These error estimates seem to differ from the unbiased standard errors only by a common multiplying constant across all stations and all event m_b 's.

The bootstrap method (Efron, 1979, 1981) has been used as a means of the uncertainty assessment in the m_b estimation problem for several years (Blandford *et al.*, 1983; McLaughlin, 1986a, 1986b, 1988). We will suggest a slightly different way of using the bootstrap technique. Specifically, we propose to enlarge the pool of residuals to include all doubly censored residuals for random drawing, and to change the definition of the "censored residual". The bootstrap method can be used to confirm the aforementioned scaling relationship between the individual error estimates and the global σ of the perturbing noise.

2. MODEL ASSUMPTIONS AND GENERAL IDEAS

Consider n_e explosions recorded at some or all of n_s stations. The linear model for the j 'th station observing the i 'th event is that the magnitude Y_{ij} can be represented as

$$Y_{ij} = E_i + S_j + e_{ij} \quad (1)$$

where E_i depends on the seismic size of the explosion, S_j is the station correction term, and the raw magnitude Y_{ij} , which contains the error term e_{ij} , is computed by $(\log_{10}(A/T) + B)$ (Veith and Clawson, 1972), as the usual practice. Since adding a common constant to each E_i and subtracting the same constant from each S_j would yield another set of solutions to (1), usually the rather arbitrary assumption that $\sum S_j = 0$ is imposed to resolve the indeterminacy. The obscuring errors e_{ij} are assumed to be uncorrelated and to belong to the same probability distribution, namely a common Gaussian distribution with zero mean and variance σ^2 . The standard regression model in (1) may be written in the form

$$Y = H \theta + e, \quad (2)$$

where H is the design (or observation) matrix of dimension $n_{\text{path}} \times n_q$, θ and Y are column vectors of size $n_q \equiv n_e + n_s - 1$ and n_{path} respectively, where n_{path} is the total number of physically available observations (or equations).

For the non-censored case, Douglas' (1966) LSMF method is identical to the standard least-squares (LS) and

$$\hat{\theta}_{\text{LS}} \equiv (H'H)^{-1}H'Y. \quad (3)$$

This least-squares estimator has many optimality properties. For instance, it is unbiased, and it gives minimum variance within the class of linear unbiased estimators. It also minimizes the *residual sum of squares*:

$$RSS \equiv (Y - H\hat{\theta})(Y - H\hat{\theta})' \quad (4)$$

Furthermore, $\hat{\theta}_{LS}$ is also the Maximum-Likelihood Estimate (MLE) under the Gaussian assumption. It is very easy to compute the uncertainty by using $\text{Var}[\hat{\theta}_{LS}] = \sigma^2(H'H)^{-1}$, which is simply scaling the variance of the random perturbations by the number of observations associated with each unknown. This σ of the random perturbations turns out to be the most important factor in determining the precision of the individual m_b estimate, even in the doubly censored case.

We will assume that there are four categories of observational data that may be available in any given situation. For the n^{th} observation in category m , the observed y_{mn} will be in one of the following four categories (Blandford and Shumway, 1982):

$m = 0$

denotes an observation y_{0n} which is available.

$m = 1$

denotes an observation y_{1n} , known only to be below some threshold level t_{1n} ; $y_{1n} \leq t_{1n}$.

$m = 2$

denotes an observation y_{2n} , known only to be above some threshold level t_{2n} ; $y_{2n} \geq t_{2n}$.

$m = 3$

denotes the case where y_{3n} is not observed as in the case of a station not recording a particular event.

Throughout this study, we will assume that there are n_0 , n_1 , n_2 , and n_3 paths associated to these four categories, respectively. Obviously, $n_0 + n_1 + n_2 + n_3 = n_e \times n_s$; and $n_0 + n_1 + n_2 = n_{\text{path}}$. We will use y_0 , t_1 , and t_2 to denote the collection of type 0, 1, and 2 observations

respectively. It is not difficult to derive an estimator for the doubly censored linear model such that the estimator would coincide with LSMF whenever it is applied to a non-censored data set. For instance, simply taking the LSMF and ignoring all censored observations is an obvious yet uninteresting case. Any nontrivial generalization of the LSMF to the censored model should at least possess some kind of optimality property, or it should seem natural. It seems very difficult to develop a procedure which can retain all the optimality properties that the LSMF has in the non-censored case, *e.g.*, unbiasedness, least-squares, and maximum-likelihood. Henceforth, we will develop a collection of estimators based on some general idea, and then impose an extra constraint to make the solution optimal in some sense.

For notational convenience we will define

$$\mu \equiv H\theta. \quad (5)$$

Let σ be the standard deviation of the independent Gaussian errors e_{ij} in equation (1), and consider

$$\phi(u) \equiv \frac{1}{\sqrt{2\pi}} \exp\left(-\frac{u^2}{2}\right), \quad (6a)$$

$$\Phi(u) \equiv \int_{-\infty}^u \phi(x) dx, \quad (6b)$$

and

$$S(u) \equiv \frac{\phi(u)}{\Phi(u)}. \quad (6c)$$

Suppose that σ is known, and suppose that the current (*i.e.*, the r^{th} step) estimate for θ is θ_r . Then the conditional expectations of the censored observations based on current estimates of the system parameters are the following:

$$E_r(Y_{0j} \mid Y_{0j} = t_{0j}) = t_{0j}, \quad (7a)$$

$$E_r(Y_{1j} \mid Y_{1j} \leq t_{1j}) = \mu_{1j}^r - \sigma S(z_{1j}) \quad (7b)$$

$$E_r(Y_{2j} \mid Y_{2j} \geq t_{2j}) = \mu_{2j}^r + \sigma S(-z_{2j}) \quad (7c)$$

where E_r denotes expectation with respect to the parameter guesses at the current stage, and

$$z_{ij} \equiv \frac{t_{ij} - \mu_{ij}^r}{\sigma}, \quad i = 1, 2; \quad j = 1, 2, \dots, n_i \quad (8)$$

In both the ILS and MLE procedures, the conditional expectations in formula (7) (*i.e.*, the "best fill-in" option as discussed in Gleit (1985)) are then used to obtain the updated coefficients θ by standard regression, *i.e.*,

$$\theta_{r+1} = (H'H)^{-1}H'Y^r \quad (9)$$

where Y^r denotes the data vector Y with conditional expectations replacing the censored values (Schmee and Hahn, 1979; Aitkin, 1981; Blandford and Shumway, 1982).

Procedures (7) through (9) are repeated until the parameter estimate, θ_r , converges. In the non-censored case, neither the iteration nor the *a priori* information about σ is required, since σ is uniquely determined as the RMS residual after a single regression on the original type 0 data. However, this is no longer the case for censored models. For an arbitrary σ , a $\hat{\theta}$ can always be found with the iteration procedure discussed above, whenever the non-detection and the clips are present. Therefore it is necessary to impose some extra constraint to make the solution unique and optimal. Two typical constraints on σ will be discussed.

θ in Equation (9) can be solved through direct inversion, or equivalently, it can be computed by stacking the equations due to the specific form of the observation model (1) (Blandford and Shumway, 1982). In fact, stacking the equations (*i.e.*, network averaging) would be much more efficient and more accurate than the cumbersome matrix algebra. To adopt this approach, the purely predicted values for type 3 paths defined as

$$E(Y_{3j} \mid Y_{3j} \text{ is missing}) = \mu_{3j}^I \quad (10)$$

must also be included in the stacking.

Note that in each iteration loop, the regression procedure (9) is carried out with the "refined" data set Y^r (Equation (7)), in which we have explicitly assigned the equal weight to each transformed path ((7b) and (7c)) as well as each regular signal (7a). In fact, the observation matrix H in equation (2) treats censored paths just the same as regular paths. Therefore it seems reasonable to define the precision in each parameter estimate by dividing σ by the square root of the total number of paths associated with that specific parameter. This is exactly the same logic used in the case of the non-censored model. We will apply this idea to both the ILS and the MLE, and check the validity of this approach by the bootstrap method in a later section.

3. ITERATIVE LEAST SQUARE METHOD

In the non-censored case, LSMF minimizes the residual sum of squares (equation 4). For the censored case, we define the "squared penalty loss" as

$$\Delta(\sigma) \equiv (\hat{Y} - H\hat{\theta})'(\hat{Y} - H\hat{\theta}), \quad (11)$$

where $\hat{\theta} = \hat{\theta}(\sigma)$ is the parameter estimate determined by a fixed σ using the iterative procedures described in the last section, and \hat{Y} the final data vector with censored values replaced by the conditional expectations (*cf.*, Equation 7). In other words, $\Delta(\sigma)$ is the sum of all squared discrepancies between the regressed parameters (*i.e.*, the mean) and the "best guess" of the observational data based on the censoring information. Obviously $\Delta(\sigma)$ can be considered as a measure of the goodness of fit. In the non-censored case (4), $\Delta = \text{RSS}$, and there exists a unique $\hat{\sigma}$ such that $\Delta = n_0 \hat{\sigma}^2$. Furthermore, substituting any other value of σ into (7) through (9) will not affect the result. In fact, this unique $\hat{\sigma}$ is simply the root-mean-squared (RMS) residuals. Along the same line of thought, there exists a unique $\hat{\sigma}$ such that

$$\Delta(\hat{\sigma}) = n_{\text{path}} \hat{\sigma}^2, \quad (12)$$

where $n_{\text{path}} \equiv (n_0 + n_1 + n_2)$. Thus this $\hat{\sigma}$ can be visualized as the generalized "root-mean-squared-residuals" for the censored model in a very loose sense. The corresponding estimator is tentatively called the Iterative Least Square (ILS). Since this σ is not known, it must be solved together with the θ . This ILS scheme is very similar to that in Schmee and Hahn (1979) and Aitkin (1981) except that they use $n_{\text{path}} - n_q$ in (12). The reason for this modification will become clear in a later section.

The ILS condition $\Delta = (n_0 + n_1 + n_2) \sigma^2$ implies the following simpler form, which is appropriate for solving σ iteratively:

$$\sigma^2 = \frac{\sum_{j=1}^{n_0} (y_{0j} - \mu_{0j})^2}{n_0 + n_1 + n_2 - \sum_{j=1}^{n_1} S(z_{1j})^2 - \sum_{j=1}^{n_2} S(-z_{2j})^2} \quad (13)$$

It is solved iteratively as follows: starting with the initial guess of θ and σ^2 (e.g., by treating the censored data as uncensored, or using non-censored data alone), the conditional expectations are calculated (Equation (7)) and a new θ is obtained. Then σ^2 is updated with (13) and the procedure is repeated until σ^2 and θ converge. Note that $S(z_{1j})$ and $S(-z_{2j})$ on the right-hand side of (13) are computed with the current estimate of σ , i.e. σ_r , while σ on the left-hand side is the updated one, i.e. σ_{r+1} .

A correction for the degrees of freedom (D.O.F.) of the whole system is suggested for application to the limit of σ_{r+1} in (13):

$$\hat{\sigma}_{ILS}^2 = \frac{n_{\text{path}}}{n_{\text{path}} - n_q} \lim(\sigma_{r+1}^2) \quad (14)$$

For the non-censored models, this D.O.F. adjustment will convert the conventional RMS residual to the unbiased σ estimate of the obscuring noise. For censored data, the adjustment in (14) is conjectured to be able to reduce substantially the bias in σ , although a (closed form) full correction for the bias is not available yet (Schmee and Hahn, 1979; Aitkin, 1981). We will show that $\hat{\sigma}_{ILS}$ differs from the bootstrap σ only by a multiplicative constant.

4. MAXIMUM-LIKELIHOOD METHOD

Suppose we seek the Maximum-Likelihood Estimates (MLE) instead of the least-squares solution, *i.e.*, we look for the parameter estimates which maximize the following log-likelihood function of the "incomplete data sampler" y_0, t_1, t_2 :

$$\begin{aligned} \ln L(y_0, t_1, t_2 \mid \theta, \sigma^2) = & -\frac{n_0}{2} \ln(2\pi\sigma^2) - \frac{1}{2\sigma^2} \sum_{j=1}^{n_0} (y_{0j} - \mu_{0j})^2 \\ & + \sum_{j=1}^{n_1} \ln \Phi(z_{1j}) + \sum_{j=1}^{n_2} \ln \Phi(-z_{2j}) \end{aligned} \quad (15)$$

where z_{ij} , Φ , ϕ , and S are defined earlier.

A number of procedures may be used to maximize the log-likelihood function, such as Newton-Raphson, or scoring. If the dimension of θ is large, then these methods become computationally intractable.

Differentiating (15) with respect to σ and setting the derivative equal to zero, one sees that σ^2 must satisfy the following condition (Aitkin, 1981):

$$\sigma^2 = \frac{\sum_{j=1}^{n_0} (y_{0j} - \mu_{0j})^2}{n_0 + \sum_{j=1}^{n_1} S(z_{1j})z_{1j} - \sum_{j=1}^{n_2} S(-z_{2j})z_{2j}} \quad (16)$$

Similar to (13) for the ILS method, (16) is solved iteratively with the Expectation Maximization (EM) algorithm (Dempster *et al.*, 1977): the "incomplete data" (*i.e.*, the censored observations) in the sufficient statistics are replaced at each iteration by their conditional expectations (7), given the observed data and the current parameter estimates, θ_r and σ_r , (the "E" step). New parameter estimates θ_{r+1} are then obtained from the replaced sufficient statistics as if they had come from a complete sample, and then substituted into (16) to solve for

the updated σ_{r+1} (the "M" step). The EM algorithm has been applied to many different research fields recently (e.g. Shumway, 1982; Shumway and Azari, 1988). Blandford and Shumway (1982) used an equivalent yet more complicated formulation of (16).

Once the iteration loop converges, i.e. $\sigma_{r+1} \approx \sigma_r$, the same D.O.F.-adjustment (14) is suggested as in the ILS case for consistency.

Note that in the non-censoring case, $n_1 = n_2 = 0$, both equation (16) and equation (13) will become the conventional RMS residual:

$$\sigma^2 = \frac{\sum_{j=1}^{n_0} (y_{0j} - \mu_{0j})^2}{n_0} \quad (17)$$

There is an easy way to distinguish the ILS and the MLE. Recall that "squared penalty loss" Δ was defined as $(\hat{Y} - H\hat{\theta})'(\hat{Y} - H\hat{\theta})$, where $\hat{Y} \equiv E(Y|y_0, t_1, t_2)$. The ILS chooses Δ/n_{path} as σ^2 , while the MLE chooses $E[(Y - H\hat{\theta})'(Y - H\hat{\theta}) | y_0, t_1, t_2] / n_{\text{path}}$. Since the computation of conditional expectation is not commutative, the ILS and the MLE will end up with different estimates of σ , and hence all the event magnitudes and station effects as well as their associated uncertainty estimates will be different in general.

EXAMPLE 1

To illustrate how the EM and the ILS methods can be used directly to estimate the uncertainty associated with their corresponding optimum parameter estimates, we have selected the same four events as in Blandford and Shumway (1982). The epicenters of these events are listed in Table 1. Table 2 gives the raw magnitude data recorded at 71 WWSSN stations that we used. It also lists the estimated station terms, \hat{S}_j , using the LSMF, the ILS,

and the MLE methods. The errors in $\hat{\theta}_{ILS}$ and $\hat{\theta}_{MLE}$ are computed with the same way as for LSMF, namely $\text{Var}\{\hat{\theta}\} = \sigma^2(H'H)^{-1}$.

Date	Name	Latitude	Longitude
631026	Shoal	39.200n	118.380w
660602	Piledriver	37.230n	116.060w
631020	Rubis	24.000n	5.000e
650227	Saphir	24.060n	5.030e

	Shoal	Piledriver	Rubis	Saphir	LSMF	ILS	MLE
AAE	----	----	5.29	5.81	-0.08±0.18	-0.08±0.19	-0.08±0.20
AAM	5.09	5.65	5.29	----	-0.02±0.15	0.09±0.16	0.10±0.17
AKU	----	5.27	----	6.08	0.04±0.18	0.06±0.19	0.06±0.20
ALQ	----	----	5.85	5.96	0.28±0.18	0.27±0.19	0.27±0.20
ANT	<4.71	5.86	5.44	5.76	0.09±0.15	0.03±0.14	0.03±0.14
AQU	<4.97	----	>5.10	5.89	0.16±0.25	0.04±0.16	0.04±0.17
ARE	5.05	5.92	5.45	5.74	0.08±0.13	0.16±0.14	0.16±0.14
ATL	5.12	5.61	6.08	----	0.24±0.15	0.35±0.16	0.36±0.17
ATU	<6.06	----	5.51	>5.58	-0.01±0.25	0.06±0.16	0.06±0.17
BHP	<4.64	<5.23	6.01	6.01	0.39±0.18	0.04±0.14	0.04±0.14
BLA	5.08	5.50	----	5.92	0.06±0.15	0.16±0.16	0.17±0.17
BOG	<4.99	5.27	<5.14	----	-0.26±0.25	-0.36±0.16	-0.37±0.17
BOZ	----	----	5.81	6.06	0.31±0.18	0.30±0.19	0.30±0.20
BUL	----	----	5.45	5.58	-0.11±0.18	-0.12±0.19	-0.12±0.20
CAR	5.55	5.71	5.08	5.32	-0.04±0.13	0.04±0.14	0.04±0.14
CHG	----	----	----	5.67	-0.06±0.25	-0.10±0.27	-0.10±0.29
CMC	----	5.00	----	5.54	-0.36±0.18	-0.34±0.19	-0.34±0.20
COL	----	5.73	----	4.65	-0.44±0.18	-0.42±0.19	-0.42±0.20
COP	<5.13	<5.61	5.44	<5.56	-0.08±0.25	-0.23±0.14	-0.24±0.14
DAL	----	----	5.55	5.79	0.05±0.18	0.04±0.19	0.04±0.20
DUG	----	----	5.47	5.73	-0.03±0.18	-0.03±0.19	-0.03±0.20
ESK	----	<5.28	----	5.87	0.14±0.25	-0.11±0.19	-0.12±0.20
FLO	4.98	----	----	5.99	0.09±0.18	0.21±0.19	0.21±0.20
GDH	<4.99	<5.29	6.01	6.14	0.45±0.18	0.16±0.14	0.16±0.14
GEO	<5.44	5.40	6.08	5.69	0.13±0.15	0.15±0.14	0.15±0.14
GIE	----	5.57	----	----	0.04±0.25	0.11±0.27	0.11±0.29
GOL	----	----	5.05	5.14	-0.53±0.18	-0.54±0.19	-0.54±0.20
JER	----	----	----	6.25	0.52±0.25	0.48±0.27	0.48±0.29
KEV	<5.03	5.34	5.68	>6.26	-0.01±0.18	0.17±0.14	0.17±0.14
KIP	5.47	6.10	----	----	0.49±0.18	0.66±0.19	0.67±0.20
KOD	----	----	----	5.39	-0.34±0.25	-0.38±0.27	-0.38±0.29
KON	<4.92	5.78	5.38	5.98	0.12±0.15	0.09±0.14	0.09±0.14
KTG	4.95	5.90	<4.96	5.22	-0.08±0.15	-0.14±0.14	-0.14±0.14
LON	----	----	<5.10	5.61	-0.12±0.25	-0.35±0.19	-0.36±0.20
LOR	----	5.78	----	----	0.25±0.25	0.32±0.27	0.32±0.29

Table 2. (Continued)

	Shoal	Piledriver	Rubis	Saphir	LSMF	ILS	MLE
LPB	5.06	----	5.22	5.47	-0.19±0.15	-0.10±0.16	-0.10±0.17
LPS	----	5.29	5.22	----	-0.27±0.18	-0.23±0.19	-0.23±0.20
LUB	----	----	----	6.44	0.71±0.25	0.67±0.27	0.67±0.29
MAL	<4.91	5.35	----	----	-0.18±0.25	-0.15±0.19	-0.15±0.20
MDS	5.07	----	5.37	5.55	-0.11±0.15	-0.02±0.16	-0.02±0.17
MNN	4.42	----	5.40	5.73	-0.25±0.15	-0.17±0.16	-0.17±0.17
NAI	----	----	5.43	>5.86	-0.09±0.25	0.09±0.19	0.10±0.20
NAT	----	5.84	----	----	0.31±0.25	0.38±0.27	0.38±0.29
NDI	----	----	5.29	5.64	-0.16±0.18	-0.17±0.19	-0.17±0.20
NNA	<4.45	5.64	5.42	5.86	0.05±0.15	-0.06±0.14	-0.06±0.14
NOR	----	5.05	----	5.23	-0.49±0.18	-0.47±0.19	-0.47±0.20
NUR	<4.72	5.36	5.12	5.42	-0.29±0.15	-0.29±0.14	-0.30±0.14
OGD	5.08	5.10	----	5.66	-0.16±0.15	-0.06±0.16	-0.06±0.17
OXF	----	5.98	----	----	0.45±0.25	0.52±0.27	0.52±0.29
PEL	----	5.47	----	6.07	0.14±0.18	0.16±0.19	0.16±0.20
POO	----	----	----	5.64	-0.09±0.25	-0.13±0.27	-0.13±0.29
PRE	----	----	5.30	5.44	-0.26±0.18	-0.26±0.19	-0.26±0.20
PTO	----	5.31	5.32	5.69	-0.15±0.15	-0.14±0.16	-0.14±0.17
QUE	----	----	4.70	4.93	-0.81±0.18	-0.82±0.19	-0.82±0.20
RCD	----	----	6.72	6.45	0.96±0.18	0.95±0.19	0.95±0.20
SCP	4.81	4.97	5.52	5.76	-0.19±0.13	-0.11±0.14	-0.11±0.14
SDB	----	----	----	5.78	0.05±0.25	0.01±0.27	0.01±0.29
SEO	4.83	5.52	----	----	-0.12±0.18	0.05±0.19	0.06±0.20
SHA	<5.15	5.64	5.86	6.16	0.29±0.15	0.27±0.14	0.27±0.14
SHI	----	----	5.81	>5.36	0.29±0.25	0.31±0.19	0.31±0.20
SHK	----	5.49	----	----	-0.04±0.25	0.03±0.27	0.03±0.29
SHL	----	----	5.33	5.45	-0.24±0.18	-0.24±0.19	-0.24±0.20
SJG	----	5.67	----	5.83	0.12±0.18	0.14±0.19	0.14±0.20
STU	<4.86	5.46	5.90	6.19	0.26±0.15	0.19±0.14	0.19±0.14
TOL	----	5.55	----	----	0.02±0.25	0.09±0.27	0.09±0.29
TRI	<4.91	5.37	5.49	5.69	-0.08±0.15	-0.08±0.14	-0.08±0.14
TRN	<4.72	5.48	5.23	5.69	-0.13±0.15	-0.15±0.14	-0.15±0.14
UME	<4.50	5.76	5.27	5.60	-0.05±0.15	-0.13±0.14	-0.13±0.14
VAL	<5.09	<5.09	5.55	5.61	-0.05±0.18	-0.20±0.14	-0.20±0.14
WES	<4.52	4.95	5.45	5.63	-0.25±0.15	-0.28±0.14	-0.29±0.14
WIN	----	----	5.01	5.50	-0.37±0.18	-0.38±0.19	-0.38±0.20

In the first experiment, each of the LSMF, MLE, and ILS was separately used with non-censored data (*i.e.*, signals) alone. They all give the same results as shown in the LSMF row in Table 3. The 147 good paths yield an RMS residual of 0.179, and $\hat{\sigma} = 0.254$ regardless of the method used. Note that the third digit after the decimal point is actually computer-dependent.

Name	Shoal	Piledriver	Rubis	Saphir
signals	14	38	42	53
noise	20	5	3	1
clips	0	0	1	4
LSMF	5.054±0.068	5.528±0.041	5.516±0.039	5.735±0.035
MLE	4.777±0.049	5.461±0.044	5.502±0.042	5.767±0.038
ILS	4.784±0.046	5.461±0.041	5.502±0.040	5.767±0.035

When the noise and clips are added for separate MLE and ILS runs, the bias reduction then becomes quite obvious for Shoal. Since there were only a few censored paths associated with the remaining three events, their $\hat{m}_{b,LSMF}$ estimates are already quite acceptable. The m_b 's of three out of four events decrease once the censored data (mainly non-detections) are included. The \hat{m}_b of Saphire slightly increases, because there are more clips than non-detections.

If we consider $\lim(\sigma_{r+1})$ the "generalized RMS residual", and assume that the D.O.F.-adjustment is sufficient to remove the bias in the variance estimate, then the ILS appears to be able to generate a smaller standard deviation than does the MLE. It is henceforth not surprising that the error estimates in $\hat{m}_{b,ILS}$ are systematically smaller than those in $\hat{m}_{b,MLE}$ (Tables 2 and 3). However, since neither $\hat{\sigma}_{ILS}$ nor $\hat{\sigma}_{MLE}$ is proven unbiased, the error estimates in

Tables 2 and 3 are actually multiplied by an unknown constant across the four events as well as all 71 stations. This constant factor for the ILS method will be different from that for the MLE, as illustrated in the bootstrap experiments in a later section. In this example, the possibly biased estimates of the standard deviations of the perturbing noise derived by different methods are $\hat{\sigma}_{ILS} = 0.270$ (Equations (13) and (14)) and $\hat{\sigma}_{MLE} = 0.286$ (Equations (16) and (14)), respectively. The log-likelihood function (15) evaluated at $\hat{\theta}_{MLE}$ is -5.622 which is larger than that of -6.103 evaluated at $\hat{\theta}_{ILS}$, as expected.

5. BOOTSTRAP METHOD

Efron's bootstrap method (1979, 1981; also Efron and Tibshirani, 1985) has been proposed by Blandford *et al.* (1983) to estimate the uncertainty in m_b estimates and station terms. Some recent work on the magnitude estimation problem has extensively utilized this technique (McLaughlin *et al.*, 1986a, 1986b; McLaughlin, 1988).

Suppose the optimal estimates of the components of θ (*i.e.*, the collection of all \hat{E}_i and \hat{S}_j) are available by using some estimation algorithm. To apply the bootstrap method, one has to construct three pools of residuals. For a type 0 (uncensored) path, we define its "regular residual" as

$$\hat{e}_{ij} \equiv Y_{ij} - \hat{E}_i - \hat{S}_j, \quad (19)$$

where (i, j) runs through all paths of category 0.

For each noisy path (*i.e.* $E_i + S_j + e_{ij} < Y_{ij}$), the corresponding "censored residual" is defined as $\hat{e}_{ij} < t_{ij} \equiv Y_{ij} - \hat{E}_i - \hat{S}_j$. These are almost the same as the regular residuals except that the equal sign was used in equation (19). Censored residuals from clipped paths are generated in a similar way, and they are stored in the same bowl together with the "regular residuals" and the "noisy residuals". For instance, after the Veith-Clawson distance normalization, the WWSSN station AQU (42.354°N, 13.403°E, in Aquila, central Italy) reported the raw magnitudes of Shoal, Rubis, and Sapphire as <4.97, >5.10, and 5.89, respectively (Table 2). By subtracting $\hat{m}_{b_{MLE}}$ (Table 3) and $\hat{S}_{MLE}[AQU] = 0.04$ (Table 2) from these readings, we get three MLE residuals: <0.15, >-0.44, and 0.08. Note that AQU was able to report a larger reading such as Sapphire with m_b 5.89, and it was clipped at a lower clipping threshold (5.10) for Rubis, even though Rubis and Sapphire were both detonated at the same French test site in

Algeria. The same observation can be made with WWSSN station LON (46.750°N, 121.810°W, in Longmire, Washington, U.S.) (Table 2). As more events are used in the regression, this phenomenon becomes more severe in that fewer stations can maintain well-defined detection and clipping thresholds in the "magnitude" domain. The easiest way to account for such unpredictable features across a large seismic network is to model them with the interchangeable random residuals as presented here.

Now for each path (i, j), a pseudo-magnitude is constructed by perturbing its predicted value, $\hat{E}_i + \hat{S}_j$, with a randomly drawn residual $\hat{e}_{ij'}$:

$$Y_{ij}^* = \hat{E}_i + \hat{S}_j + \hat{e}_{ij'} \quad (20)$$

where (i', j') denotes the identifier of the randomly drawn event-station pair. If this residual was censored, then the equality sign in equation (20) should be replaced by < or >, according to the flag of $e_{ij'}$. Thus we are randomly allocating the residuals (with replacement) to obscure the predicted magnitude value. A good path (*i.e.* of type 0) might become clipped or noisy during certain resampling procedures, but missing paths (*i.e.* type 3 "observations") remain invariant.

The pseudo-magnitude samples are used to reconstruct new estimates \hat{E}_i^* and \hat{S}_j^* using a selected estimator. This Monte Carlo procedure is repeated many times, and the sample standard deviations of the \hat{E}_i^* 's and \hat{S}_j^* 's are proposed by Efron (1981) as good approximations to the standard errors of the original estimators \hat{E}_i and \hat{S}_j . The D.O.F.-adjustment (14) is applied to the bootstrap standard errors for consistency.

Using the combination of the MLE and the bootstrap (with 200, 400, and 600 bootstrap resamplings), the standard error estimates of the four events in Example 1 are listed in Table

4 below:

Event	std. er. 200	std. er. 400	std. er. 600	$\hat{m}_{b_{MLE+B}} - \hat{m}_{b_{MLE}}$	$\hat{\sigma}_{MLE+B}$
Shoal	0.059	0.059	0.058	0.005	0.336
Piledriver	0.049	0.052	0.053	0.009	0.345
Rubis	0.043	0.045	0.045	0.007	0.308
Saphir	0.042	0.046	0.056	0.007	0.332

In the table, std. er. i , $i=200,400,600$ represents the uncertainty estimates made with 200, 400, and 600 bootstrap resamplings, respectively. Comparing Tables 3 and 4, it is obvious that the errors in each event as estimated by the MLE with the bootstrap method are very close to what we obtained with one single call of the MLE alone. The discrepancy between the averaged $\hat{m}_{b_{MLE+B}}$ after 600 resamplings and the $\hat{m}_{b_{MLE}}$ is negligible (column 5 of Table 4). If we extract the bootstrap standard error in each station and event (the "std. er. 600" in Table 4) and multiply it by the square-root of the total number of observations associated (signals, noise, and clips), the result (column 6 of Table 4) appears to be a pretty good approximation of $\hat{\sigma}_{MLE}$. The root-mean-squared value of such $\hat{\sigma}_{MLE+B}$ computed from 71 stations and 4 events is 0.296, whereas the $\hat{\sigma}_{MLE}$ was 0.286.

We also performed the same experiment based on a combination of ILS and the bootstrap, as shown in Table 5 below:

Event	std. er. 200	std. er. 400	std. er. 600	$\hat{m}_{\text{ILS+B}} - \hat{m}_{\text{ILS}}$	$\hat{\sigma}_{\text{ILS+B}}$
Shoal	0.059	0.059	0.057	0.005	0.332
Piledriver	0.049	0.052	0.052	0.008	0.342
Rubis	0.043	0.044	0.044	0.007	0.298
Saphir	0.041	0.045	0.043	0.006	0.328

In this case, the root-mean-squared $\hat{\sigma}_{\text{ILS+B}}$ (averaged over 71 stations and 4 events) is 0.294, whereas the $\hat{\sigma}_{\text{ILS}}$ was 0.278.

Efron (1981) and McLaughlin (1988) perform the resampling among the observed data themselves, because there was only one unknown parameter and one distribution. In the situation of multivariate estimation, a centering process (to remove the mean) is necessary, and the resampling is carried out on the residuals (Blandford *et al.*, 1983).

Note that in Blandford *et al.* (1983), the resampling of the residuals is limited to the paths of type 0 only, and all clipped or noisy observations are held fixed at their threshold levels during all bootstrap iterations. The same scheme is also applied by McLaughlin (1986a, 1986b). This is based on the assumption that the same stations might tend to be noisy or clipped from event to event (Blandford *et al.*, 1983), which could be true if all events are from the same test site. For events from several test sites, we have noticed that keeping clipped and noisy paths unchanged will cause a larger discrepancy between the original optimal estimators $\{\hat{E}_i, \hat{S}_j\}$ and the averaged bootstrap estimators, and hence it will yield questionable uncertainty estimates. This observation led us to an alternative approach to treat all residuals equally, whether they are censored or not, in the resampling.

EXAMPLE 2

During the past several years, Geotech's WWSSN database has been gradually expanded to 110 events (totaling 328 usable "a", "b", and "max" event phases) (McLaughlin, 1986a; Chan *et al.*, 1988). We have separately applied the ILS, the MLE, the ILS with the bootstrap, and the MLE with the bootstrap on the complete data set.

The 328 phases were treated as uncorrelated events in the regressions. The 7547 good paths (*i.e.*, signals only) yield an RMS residual of 0.258 and $\hat{\sigma}_{LSMF}$ of 0.266. When the 5012 noisy and 950 clipped paths are added to the input data set, $\hat{\sigma}_{ILS}$ is 0.263, and $\hat{\sigma}_{MLE}$ is 0.329, roughly in accord with other work (*e.g.*, Bache, 1982; Veith and Clawson, 1972). The log-likelihood values computed at $\hat{\theta}_{ILS}$ and $\hat{\theta}_{MLE}$ are -4760 and -4325, respectively.

Figure 1 plots the log-likelihood and the squared penalty loss as a function of σ in the range from 0.10 to 1.00, for the censored data in this example. As already mentioned earlier, each σ determines a unique solution of θ through the iterations ((7)-(9)). A question of top importance is how to constrain the σ for optimality. From the log-likelihood function evaluated at every possible σ (filled circles in Figure 1), it is clear that the log-likelihood function attains its maximum at RMS $\sigma = 0.324$, or $\hat{\sigma}_{MLE} = 0.329$ after the D.O.F.-adjustment. On the other hand, the squared penalty loss function $\Delta(\sigma)$ (shown as "+" sign) has no apparent critical point in the range of interest. The ILS method picks the σ with $\Delta = (n_0+n_1+n_2) \sigma^2$, which is valid only at RMS $\sigma = 0.258$, or $\hat{\sigma}_{ILS} = 0.263$ after the D.O.F. adjustment. Since the ILS method assumes that each censored path contributes an equal amount (or weight) of information as does any non-censored path, conceptually this is already the extremal usage of the censored data, and hence no smaller σ is acceptable from a realistic

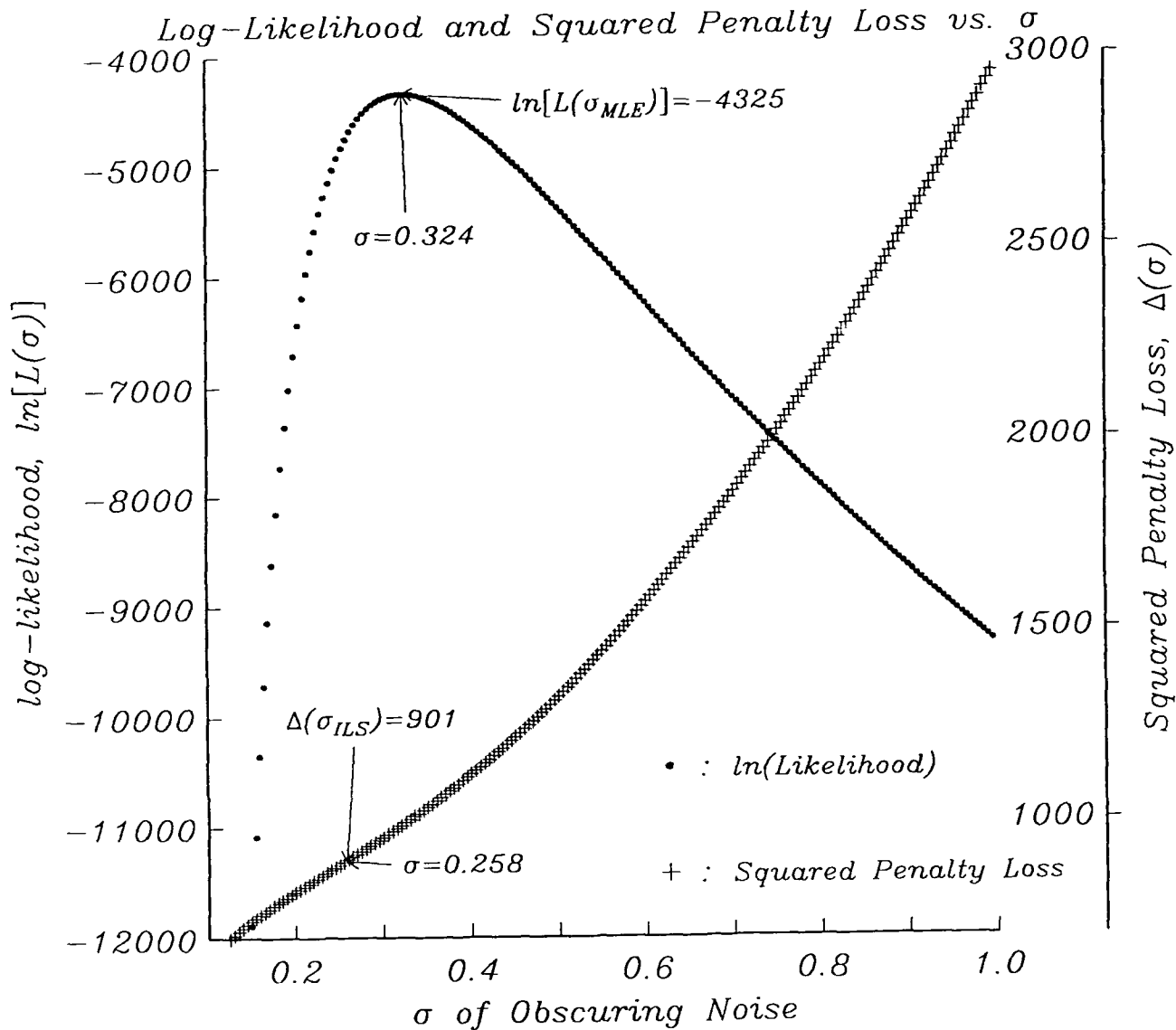


Figure 1. The log-likelihood and the squared penalty loss as a function of σ in the range from 0.10 to 1.00. The log-likelihood function attains its maximum at RMS $\sigma = 0.324$, or $\hat{\sigma}_{MLE} = 0.329$ after the D.O.F. adjustment. The squared penalty loss function $\Delta(\sigma)$ increases almost linearly as σ increases, and it has no apparent critical point in the range considered. Conceptually, censored paths cannot provide more information than the non-censored paths, and therefore the $\Delta = (n_0+n_1+n_2) \sigma^2$ determines the smallest acceptable σ , which yields RMS $\sigma = 0.258$, or $\hat{\sigma}_{ILS} = 0.263$ after the D.O.F.-adjustment. Thus ILS is indeed optimal in terms of the squared penalty loss.

point of view. Thus $\Delta(\hat{\sigma}_{ILS})$ is the smallest achievable penalty loss if we limit the σ to be no less than $\Delta/(n_0+n_1+n_2)$. In this sense, ILS is also optimal.

Figure 2a plots the $\hat{m}_{b_{MLE}}$ and $\hat{m}_{b_{ILS}}$ versus $\hat{m}_{b_{LSMF}}$ for all 110 events. In using WWSSN data, there is only a narrow magnitude range from about 5.7 to 6.4 in which the censoring effects of clipping or non-detection do not lead to serious bias (Chan *et al.*, 1988), in accord with many network studies (Ringdal, 1986; Clark, 1983; Lilwall, 1986; Lilwall *et al.*, 1988; Christoffersson and Ringdal, 1981; Chinnery, 1978; Everndon and Kohler, 1976). The discrepancies between $\hat{m}_{b_{ILS}}$ and $\hat{m}_{b_{LSMF}}$ are always slightly smaller than those between $\hat{m}_{b_{MLE}}$ and $\hat{m}_{b_{LSMF}}$. Basically this is because $\hat{\sigma}_{ILS}$ is smaller than $\hat{\sigma}_{MLE}$, and hence the ILS tends to underestimate somewhat the bias compensation in the computation of conditional expectations, as compared to the MLE (Figure 2b). The same observation can be made with the receiver effects of 127 stations (Figures 3a and 3b). Figure 3c plots the histogram of receiver effects estimated with the LSMF, the MLE, and the ILS method using bin width 0.1 unit.

The uncertainty estimates of 127 stations and 328 phases computed with the four aforementioned techniques are plotted in figures 4a and 4b. The results of 600 iterations of the ILS (or the MLE) and the bootstrap show a very clear linear relationship between $\log(\sqrt{\text{number of observations}})$ and $\log(\text{uncertainty estimate})$ (Figures 5a and 5b). This means that the uncertainty in each estimated parameter is completely determined by the total number of observations associated with that parameter, provided that the global σ is known. If $\hat{\sigma}_{ILS}$ or $\hat{\sigma}_{MLE}$ is used, instead of the true σ , then a constant multiplicative adjustment in the uncertainty estimates is necessary (Figures 5a and 5b). Conversely, the global $\sigma_{unbiased}$ can be stably estimated from any individual uncertainty estimate (by multiplying by the square-root

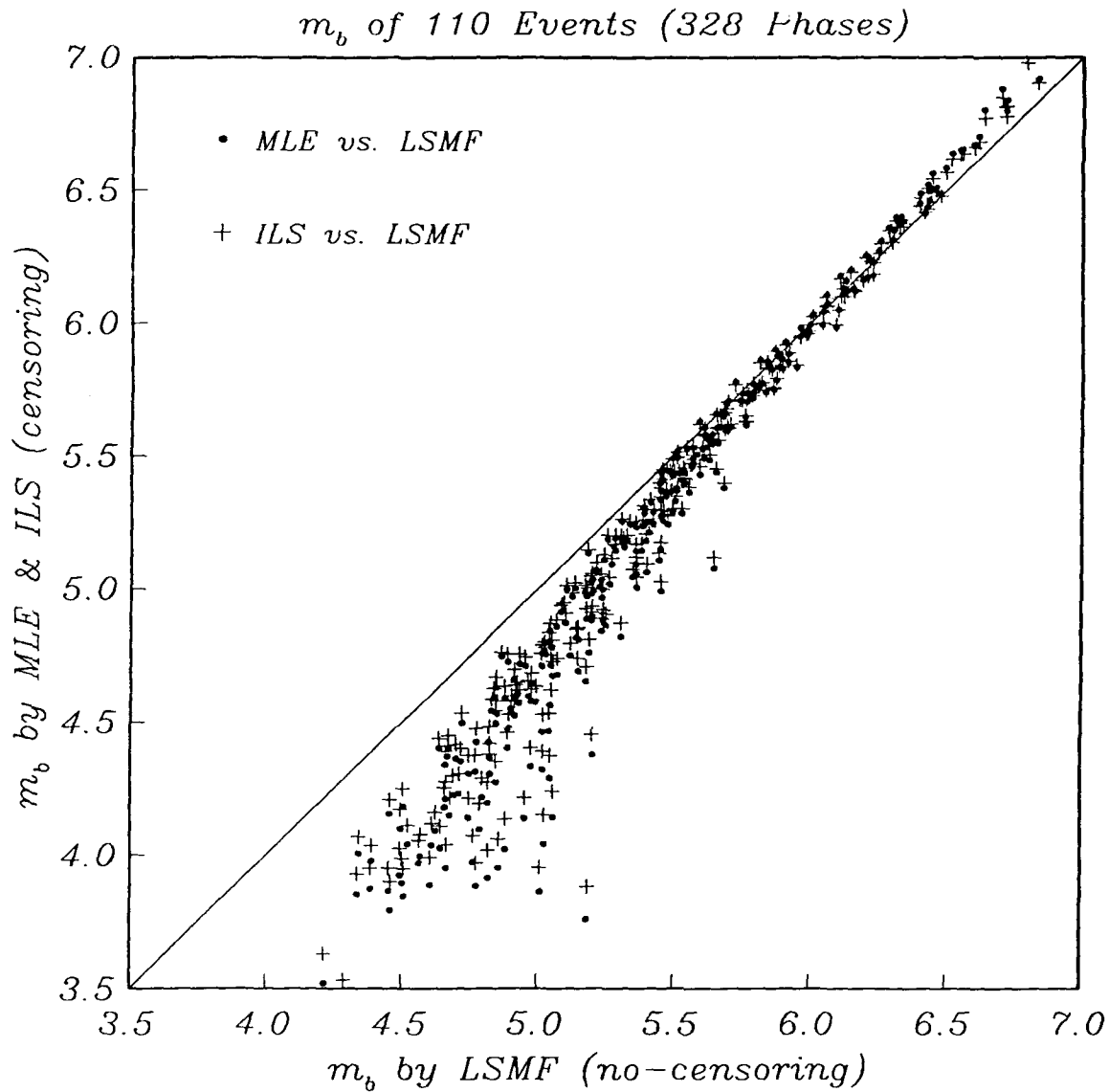


Figure 2a. The $\hat{m}_{b_{MLE}}$ and $\hat{m}_{b_{ILS}}$ versus $\hat{m}_{b_{LSMF}}$ for 110 explosions (328 phases). There is only a narrow magnitude range from about 5.7 to 6.5 in which the censoring effects of clipping or non-detection do not lead to serious bias. Compared to MLE, ILS tends to underestimate somewhat the censoring effects.

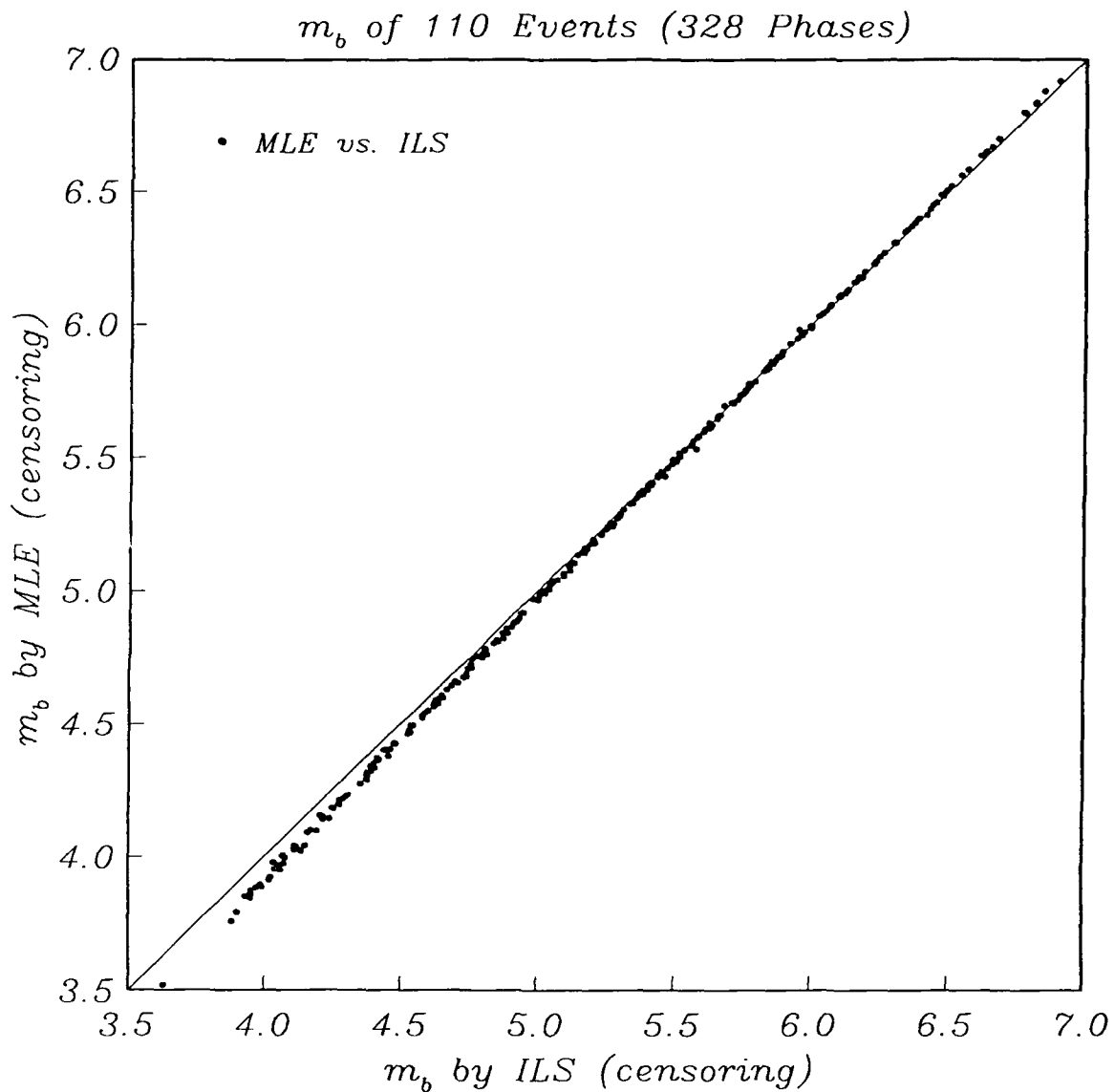


Figure 2b. The $\hat{m}_{b_{MLE}}$ versus $\hat{m}_{b_{ILS}}$ for 110 explosions (328 phases). Compared to MLE, ILS tends to underestimate somewhat the censoring effects.

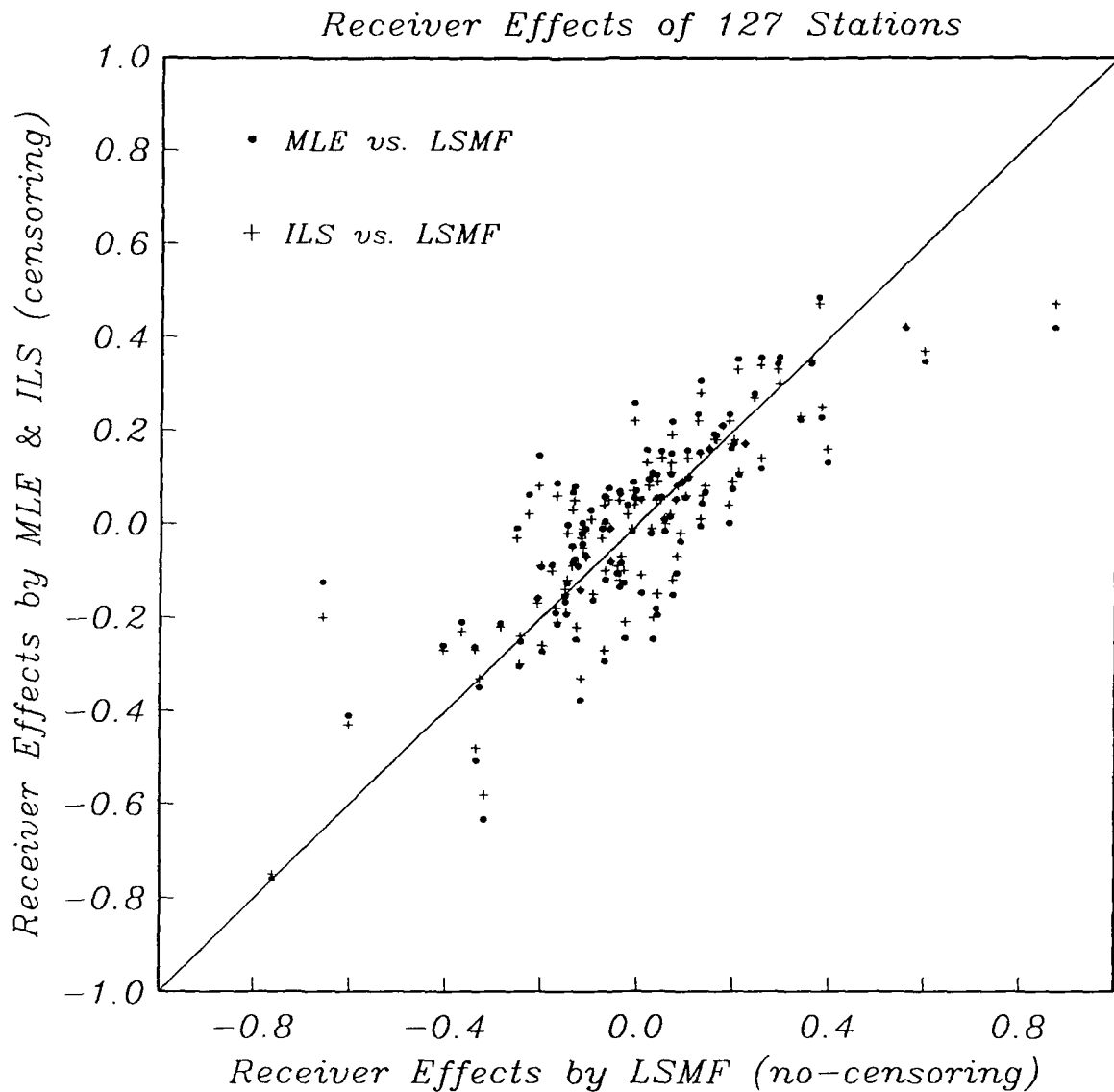


Figure 3a. The receiver effects of 127 WWSSN stations indicate that ILS tends to underestimate the censoring effects due to clippings or non-detections, same as in Figures 2a and 2b.

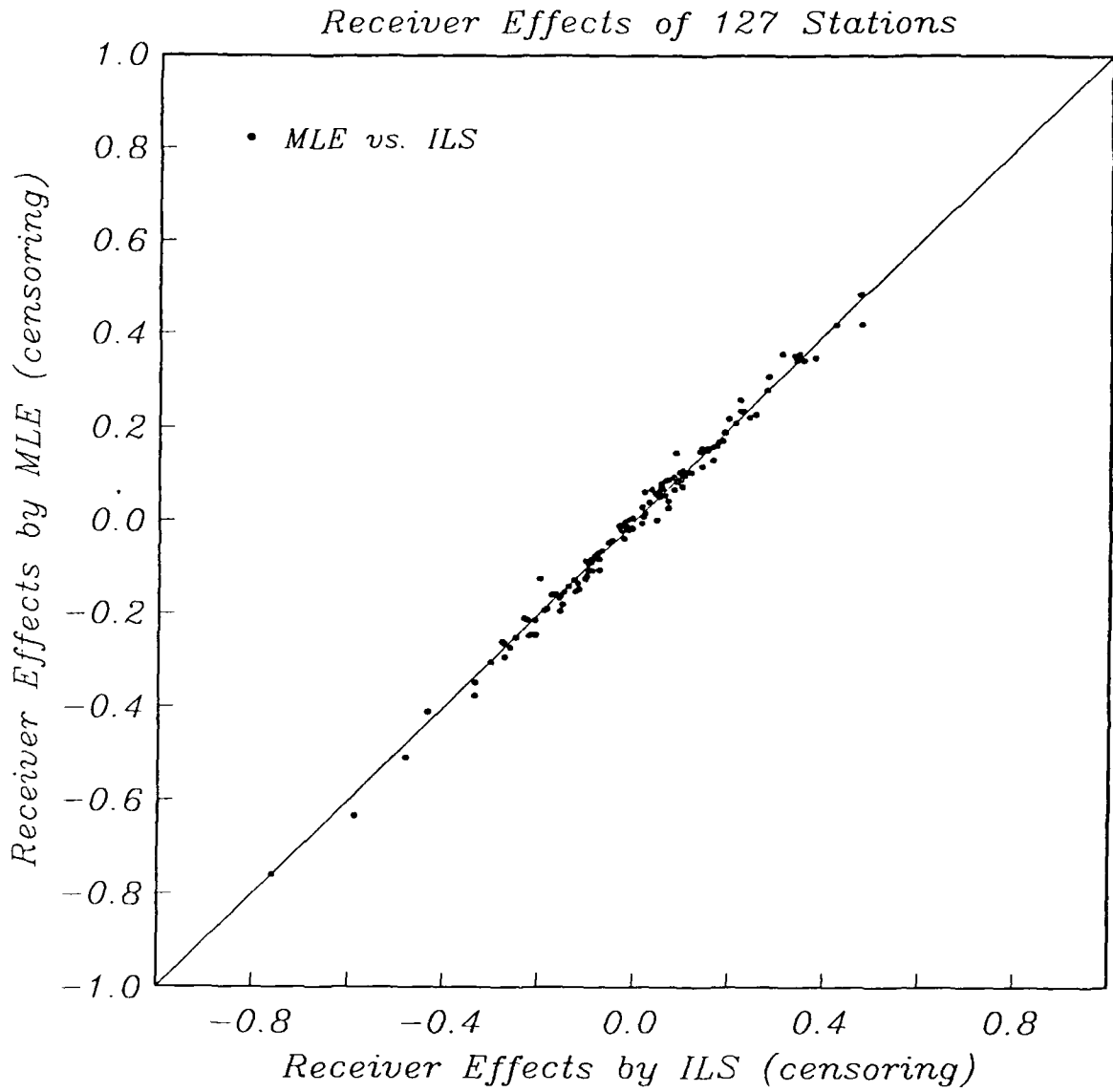


Figure 3b. Comparison of the receiver effects estimated by the MLE and the ILS.

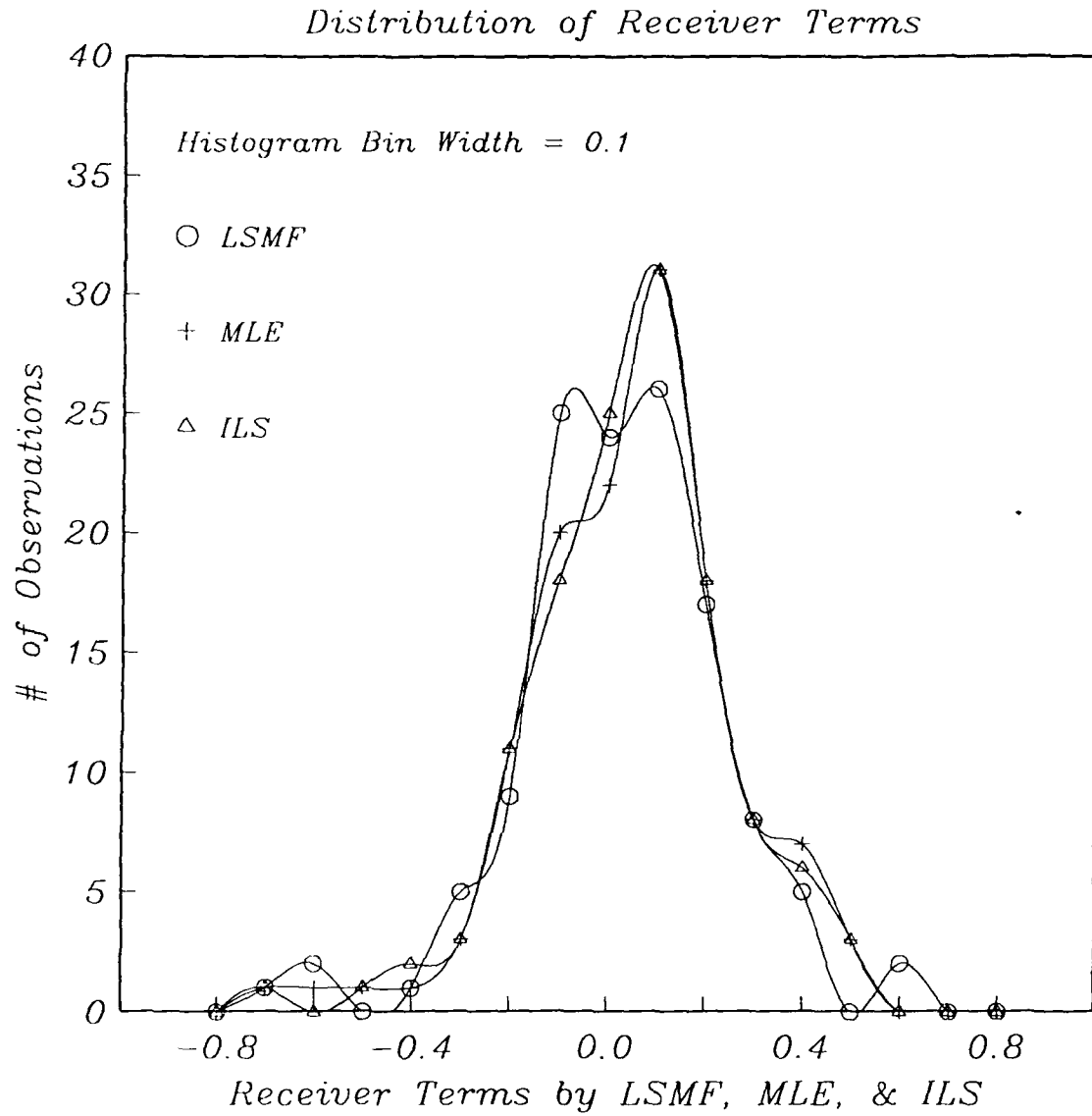


Figure 3c. Histogram of the receiver effects with bin width 0.1 unit. Circles, “+” signs, and triangles represents the spread of the 127 receiver terms estimated with the LSMF, the MLE, and the ILS methods respectively.

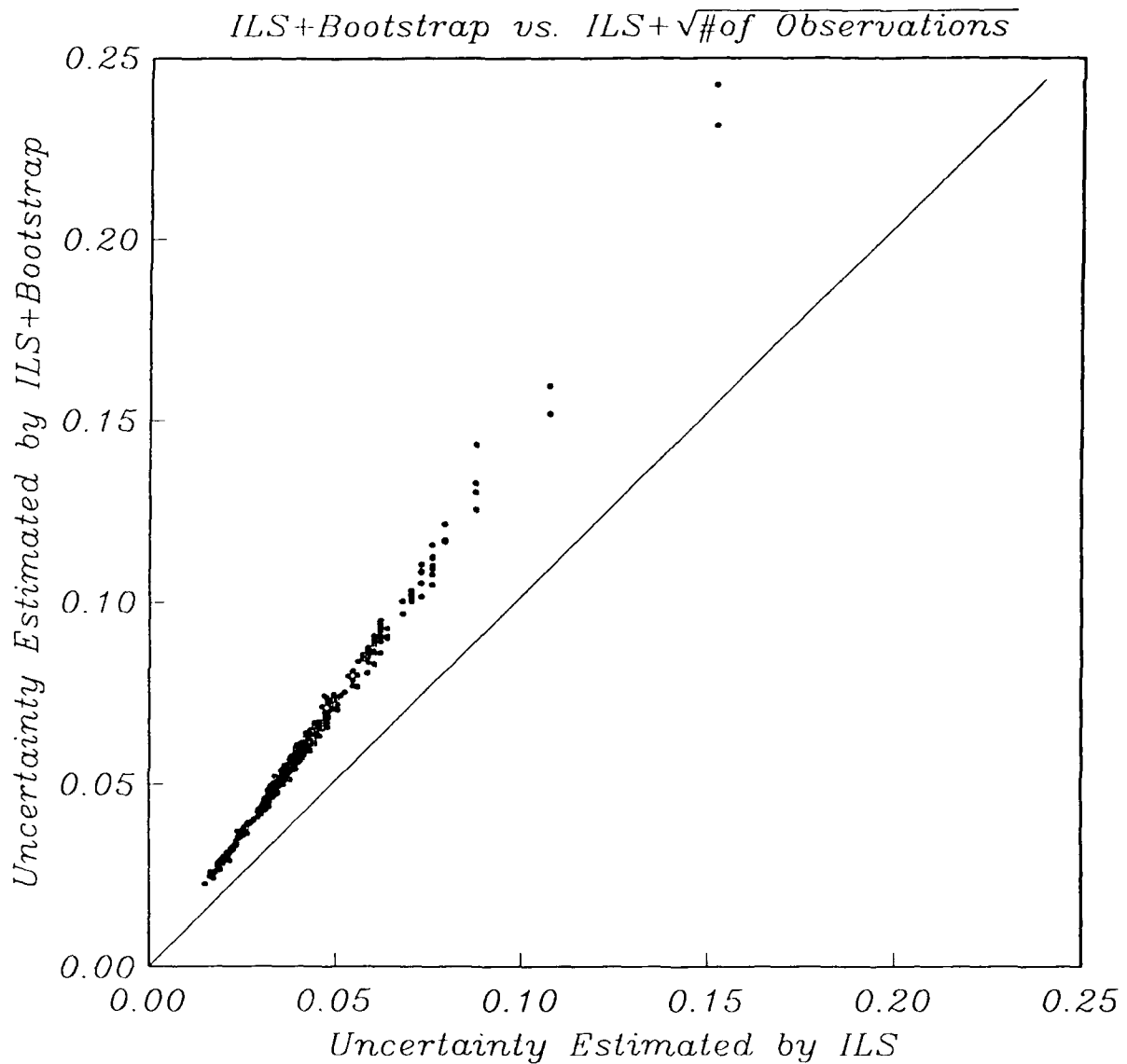


Figure 4a. The uncertainty estimated by the ILS versus that by the ILS and bootstrap. The abscissa $Error_{ILS}$ is *predicted* in an analytical manner by dividing the σ_{ILS} by the square root of number of associated observations. The ILS plus bootstrap method computes the ordinate with statistics from 600 Monte Carlo simulations. The highly linear relationship between these two methods strongly indicates that the ILS alone would give a fairly good estimate of the uncertainty, except for the constant magnifying factor (*i.e.*, the slope), 1.450.

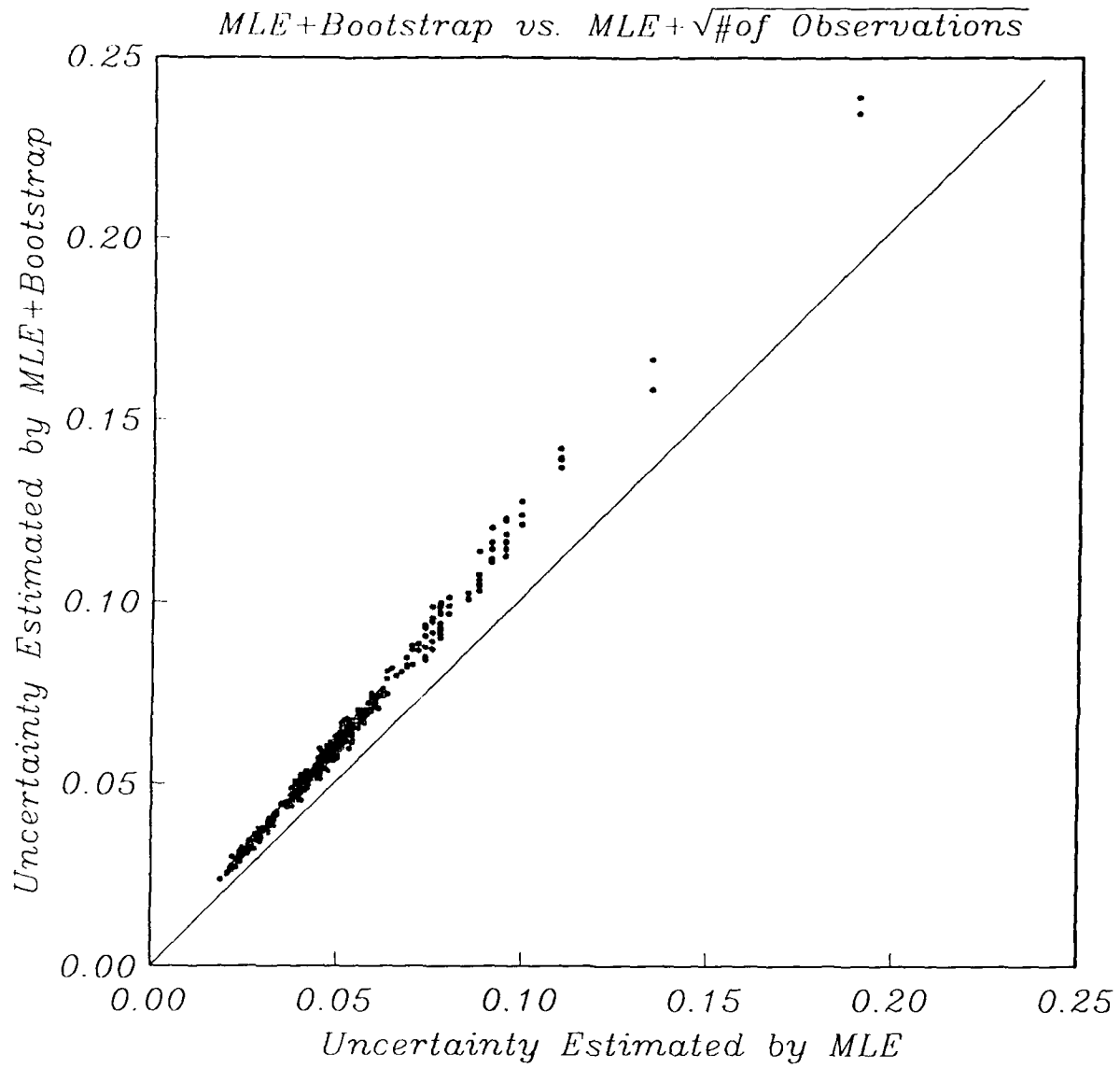


Figure 4b Same as Figure 4a except that the MLE is used instead of the ILS. The magnifying factor required in this case is 1.218.

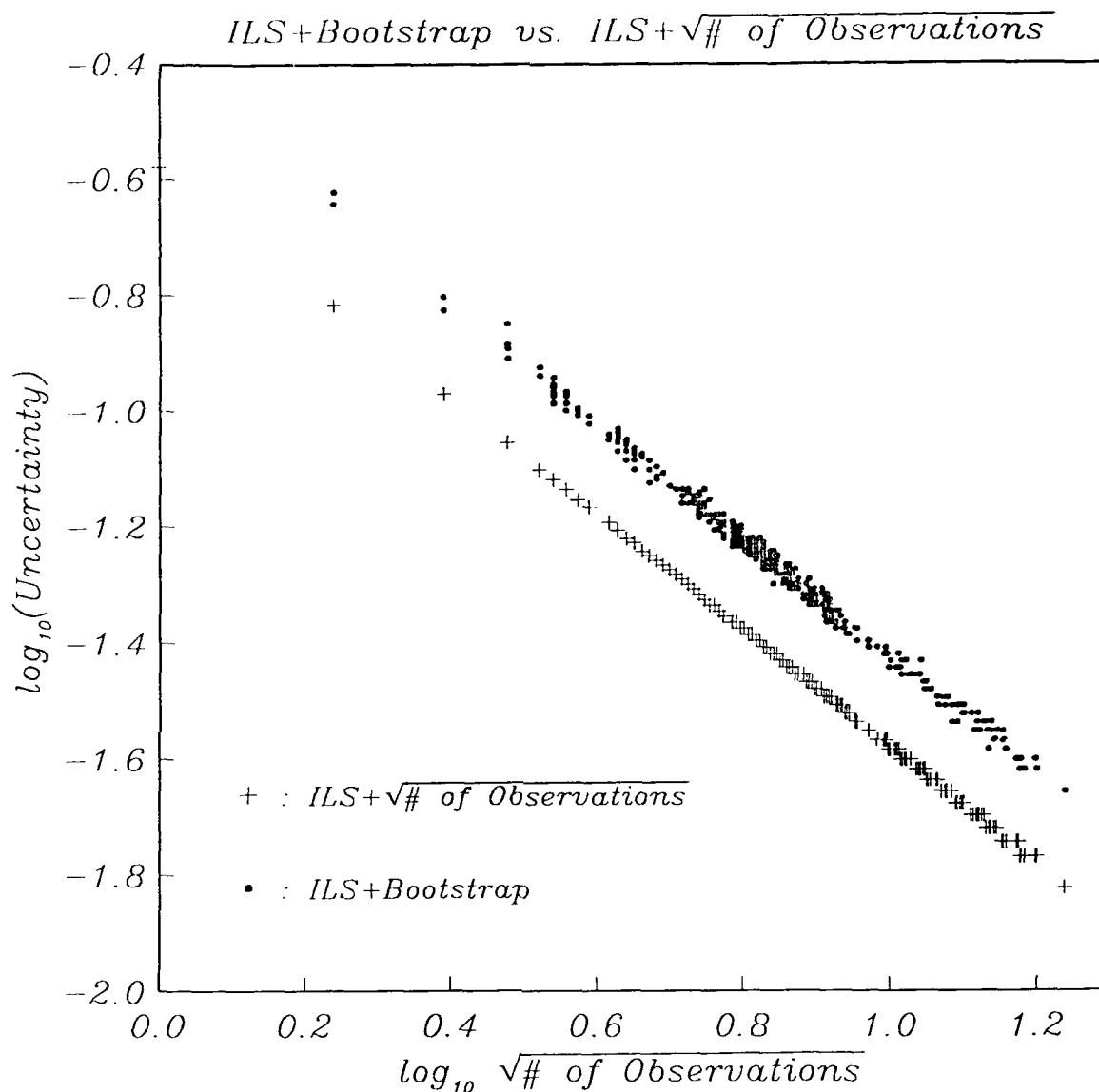


Figure 5a. The $\log_{10}\sqrt{\#}$ of observations (including signals, noises, and clips) versus the $\log_{10}(\text{uncertainty estimate})$. Filled circles represent the results from 600 bootstrap iterations. The nearly linear relationship ($X + Y \approx \log_{10}(0.381)$) indicates that the product of the $\sqrt{\#}$ of observations and the individual error estimate will be a stable estimator of the true σ of the obscuring perturbations. The lower curve ($X + Y = \log_{10}(0.263)$) gives the predicted uncertainty with $\hat{\sigma}_{ILS}$.

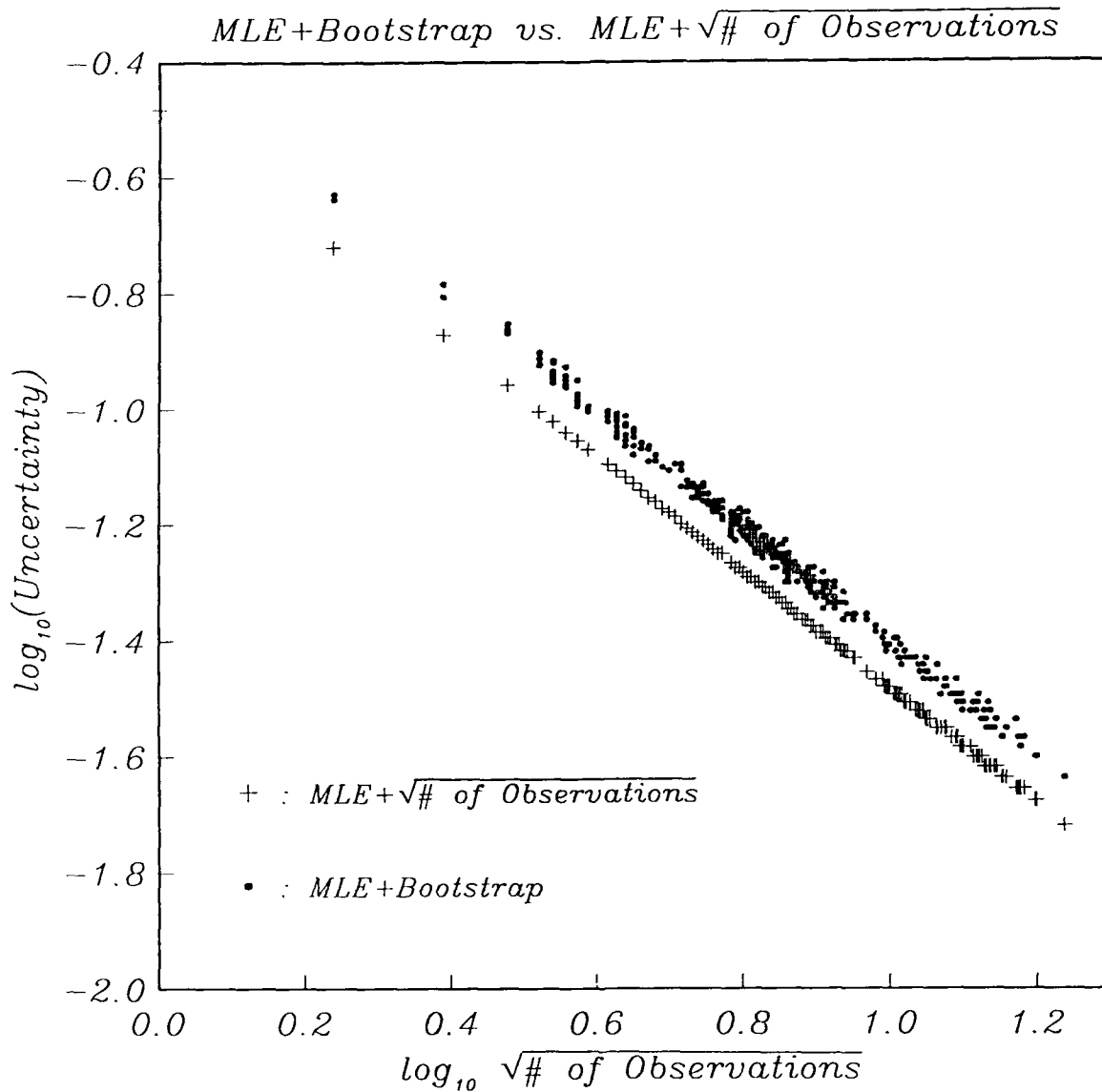


Figure 5b. Same as Figure 5a except that the MLE is used instead of the ILS. The linear relationship is as obvious as in the ILS case. The offset between the theoretical curve and the bootstrap's result is smaller than that in Fig. 5a. The upper line ($X + Y \approx \log_{10}(0.401)$) and the lower line ($X + Y = \log_{10}(0.329)$) will merge together in the non-censoring case.

of the associated number of observations). In this example, $\hat{\sigma}_{MLE+B}$ and $\hat{\sigma}_{ILS+B}$ are 0.401 and 0.381, respectively, suggesting a magnifying factor of 1.218 and 1.450 for $\hat{\sigma}_{MLE}$ and $\hat{\sigma}_{ILS}$, respectively, under the assumption that bootstrap gives a better estimate of σ (Figures 4a and 4b). In the previous example of four events, the correcting factors required were 1.035 (for the MLE) and 1.058 (for the ILS) (*cf.* the discussion following Tables 4 and 5).

Figures 6a and 6b show the histogram of the residuals corresponding to the ILS and the MLE with bin width 0.1 unit. Circles, “+” signs and triangles represent the spread of 7547 “regular residuals”, 5012 “noisy residuals”, and 950 “clipped residuals”, respectively. The ILS residuals are slightly more concentrated than those of the MLE, since $\hat{\sigma}_{ILS}$ is smaller than $\hat{\sigma}_{MLE}$. The shape of the interpolated histogram of the regular residuals empirically justifies the idealized assumption imposed on (1) that residuals follow a normal distribution. Note that the “censored residuals” are not realizations or direct observations of the Gaussian noise. They represent the “thresholds” in observing the Gaussian noise. The noisy residuals are compactly clustered on the positive side, while the clipped residuals are clustered on the negative side. Such extra bounding information would of course improve precision in estimating σ . Note that the ILS and the MLE are the standard least squares methods (9) acting on the \hat{Y} , *i.e.* the “refined observations” as defined in (7). If we define the “refined residual” as the discrepancy between the final conditional expectation of the censored observation (7) and the regressed mean, then an *equivalent* histogram of Figure 6a or 6b is obtained which shows again that the Gaussian assumption is adequate (Figure 6c). This equivalent histogram illustrates quantitatively the constructive effect of incorporating the censored information. In statistical terms, this means that the Central Limit Theorem is also valid in the case of a doubly censored model as considered in this study.

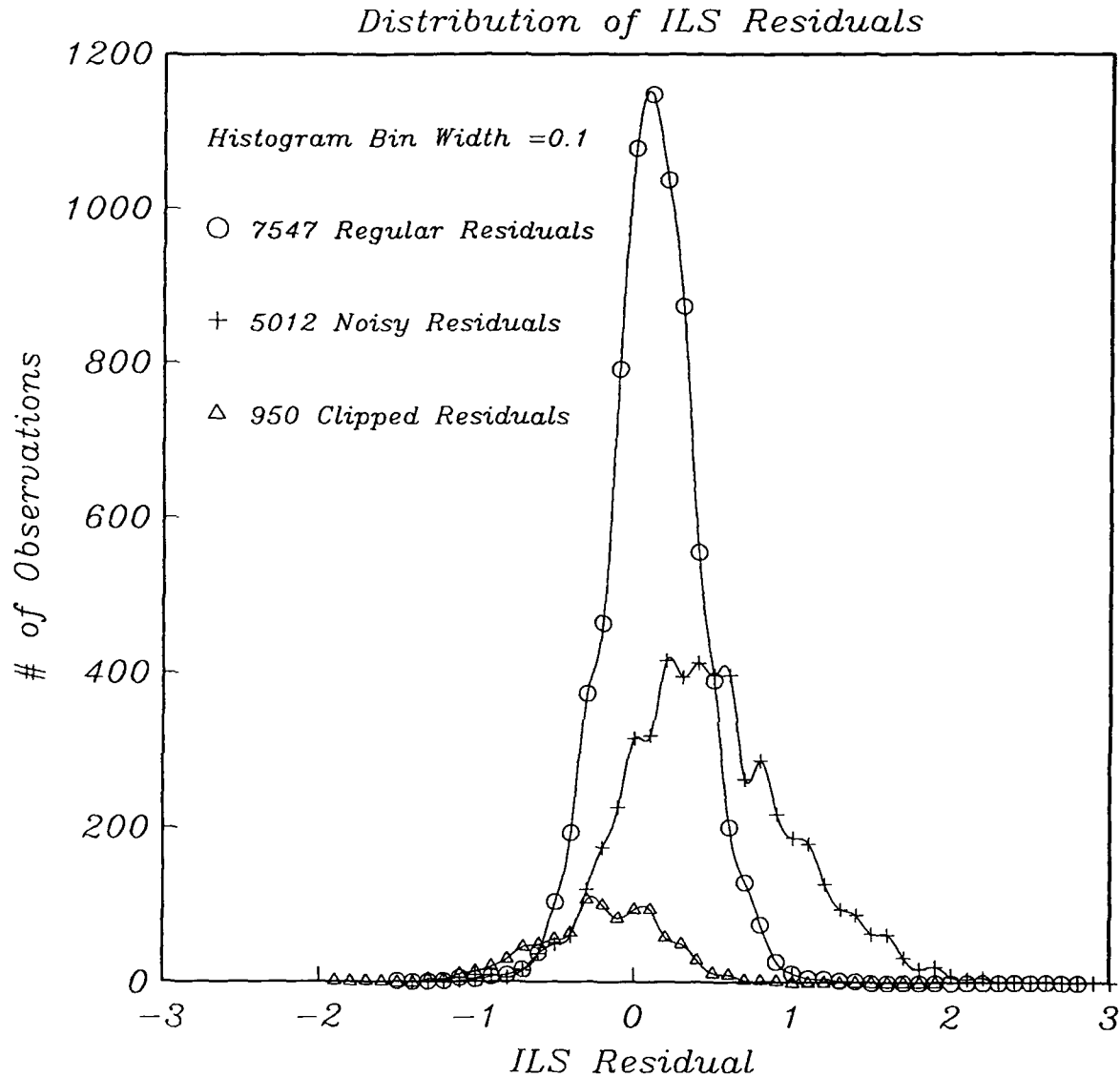


Figure 6a. The histogram of the ILS residuals with bin width 0.1 unit. Circles, “+” signs, and triangles represents the spread of 7547 “regular residuals”, 5012 “noisy residuals”, and 950 “clipped residuals”, respectively. The ILS residuals are slightly more concentrated than that of MLE, because $\hat{\sigma}_{ILS}$ is smaller than $\hat{\sigma}_{MLE}$. The shape of the interpolated histogram empirically justifies the idealized assumption that residuals follow a normal distribution.

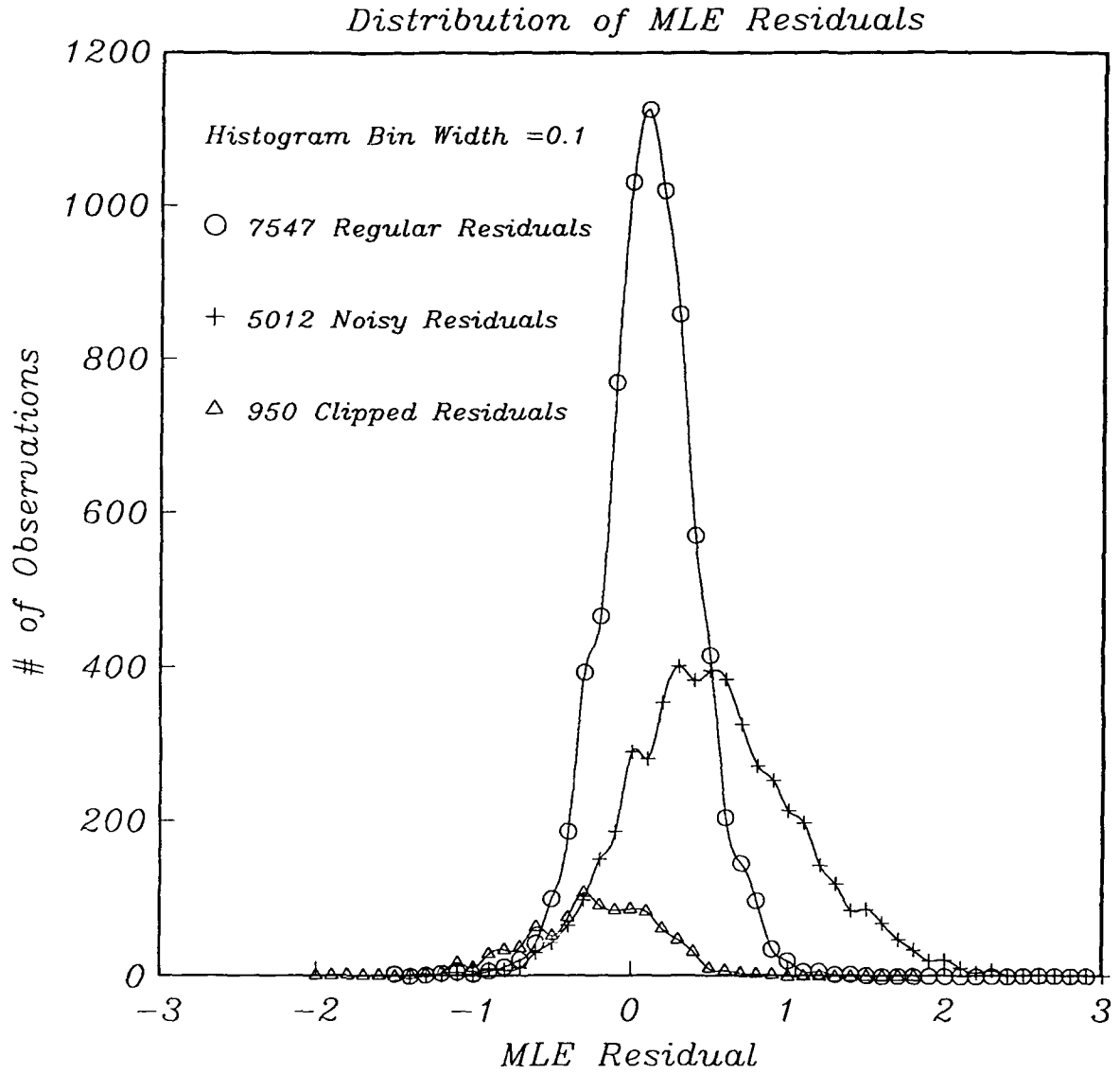


Figure 6b. The histogram of the MLE residuals (See Figure 6a for caption).

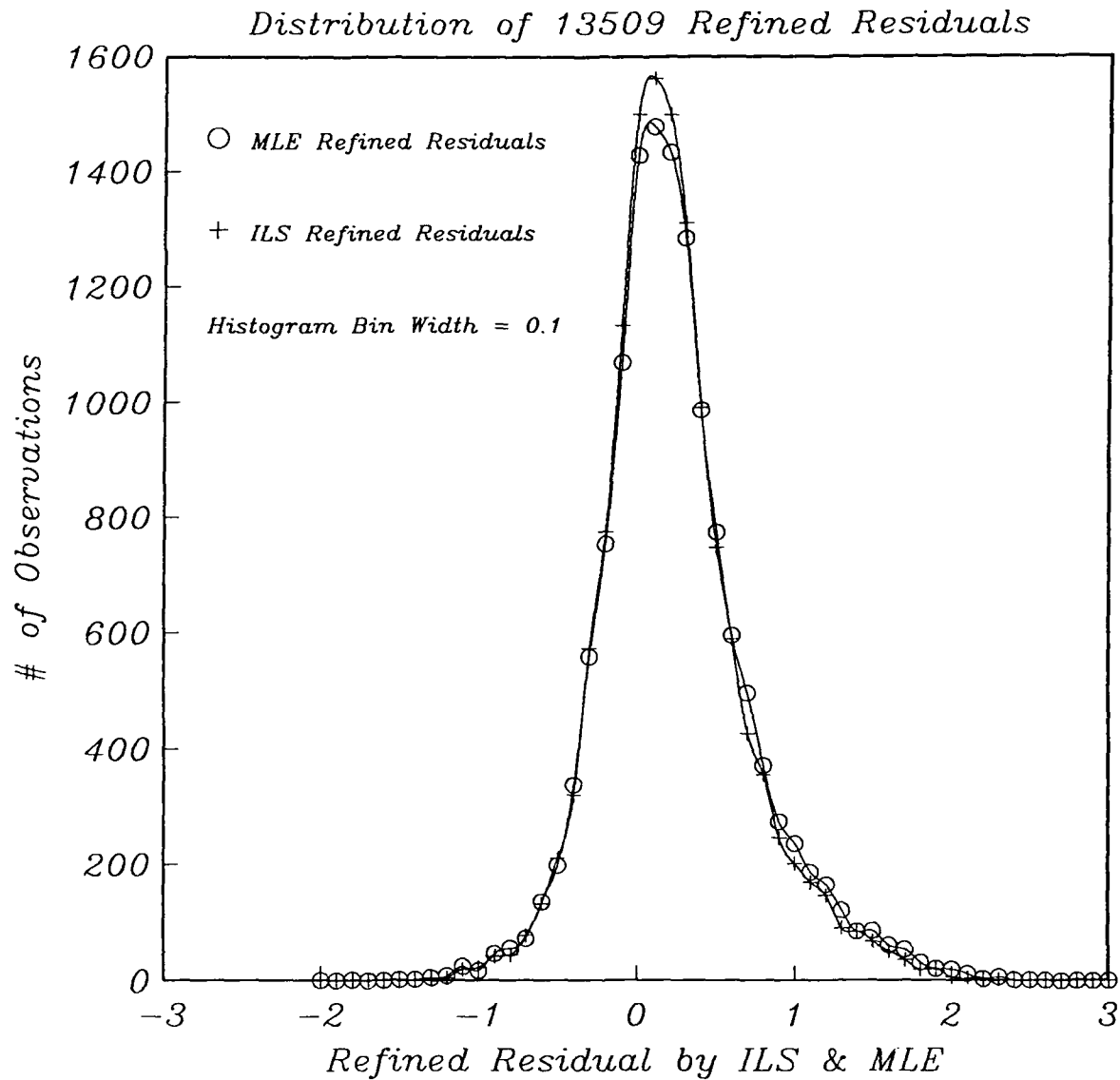


Figure 6c. The “refined” histogram showing the effect of incorporating the censored information. Here we replaced each censored residual by its “refined” form, which is defined as the discrepancy between the final conditional expectation of the censored observation and the regressed mean. The interpolated histograms illustrate again that the Gaussian assumption is adequate.

6. DISCUSSION AND CONCLUSIONS

In this study, we have briefly reviewed several methods used in network magnitude estimation, and we have illustrated that the uncertainty in the parameter estimates can be easily estimated by scaling the standard deviation of the perturbing noises. The Iterative Least-Squares method is very similar to the EM algorithm for the Maximum-Likelihood Estimator in that the same routine can be used except a minor modification to the calculation of σ (*cf.*, (13) and (16)) (Aitkin, 1981). Even though neither of these two estimators is truly unbiased for σ in statistical sense, the MLE has attracted more attention in the seismological community, at least as reflected by the literature to date.

The original ILS scheme (Schmee and Hahn, 1979; Aitkin, 1981) applies the D.O.F.-adjustment (14) on σ_r *within* each iteration loop, *i.e.* they look for the σ satisfying $\Delta = (n_{\text{path}} - n_q)\sigma^2$, while the present scheme suggests doing the D.O.F.-adjustment in an off-line sense for consistency with the MLE. Schmee and Hahn's original scheme yields a result of 0.264 for $\hat{\sigma}_{\text{ILS}}$, 909.8 for Δ , and -4677 for the log-likelihood function in Example 2, just slightly different from ours. For regression problems with small sample size such as that in Schmee and Hahn (1979) and Example 1 considered here, the discrepancy between $\hat{\theta}_{\text{ILS}}$ and $\hat{\theta}_{\text{MLE}}$ is insignificant. However, it is not true for large sample cases such as Example 2 of this study.

A few comments on the bootstrap method are worth making: the bootstrap method is computationally inefficient since it usually requires hundreds of MLE or ILS calls. The more data (and hence more residuals) that are used, the more Monte Carlo computations are required. The illustrative example given in Tables 4 and 5 is nearly the extreme case, since

the total number of unknowns is not too large. If there are thousands of residuals as in the second example, then the bootstrap method would consume copious computational time. Secondly, we have shown that each of the ILS and the EM algorithms will provide its own error estimates in a "quick and easy" manner. If the possibly biased estimate of σ is an acceptable approximation, then a single call of the ILS or the MLE will save much computational time. Thirdly, the \hat{m}_b and station estimates obtained from the bootstrap method would not be exactly identical to the LSMF (or the MLE, the ILS) even in the non-censoring case (*cf.*, Tables 4 and 5). At best, it regenerates m_b estimates asymptotic to the adopted estimator, while the "exact" result (Table 3) must have existed in order to start the bootstrap loop. Earlier work on the network (or single event) m_b estimation (*e.g.* McLaughlin *et al.*, 1986a, 1986b; McLaughlin, 1988) uses the bootstrap only for error estimation, while the m_b 's and the station terms were actually obtained from a separate call of the EM method. Efron and Tibshirani (1985) have shown that, for the simplest non-censored case, the bootstrap method is asymptotically correct yet redundant in assessing the uncertainty in the sample mean. The same conclusion seems to be valid even in the censored case, as illustrated in this study.

7. ACKNOWLEDGEMENTS

RSJ is grateful to Wilmer Rivers for his support and encouragement and to Robert Blandford, and David Boore for insightful discussions and comments. Keith McLaughlin drew RSJ's attention to the magnitude estimation problems. Wilmer Rivers, Winston Chan, Chris Lynnes, and Bob Cessaro reviewed and improved the manuscript. The data in the examples came from Geotech's WWSSN database, which were digitized and preprocessed by Robert Wagner, Margaret Marshall, R. Ahner, and James Burnetti under various projects. This research was partially supported under DARPA contract MDA903-87C-0069, monitored by Defense Supply Service, Washington. The views and conclusions contained in this paper are those of the authors and should not be interpreted as representing the official policies, either expressed or implied, of the Defense Advanced Research Projects Agency or the U.S. Government.

8. REFERENCES

- Aitkin, M. (1981). A note on the regression analysis of censored data, *Technometrics*, 23, 161-163.
- Bache, T. C. (1982). Estimating the yield of underground nuclear explosions, *Bull. Seism. Soc. Am.*, 72, S131-S168.
- Blandford, R. R., and R. H. Shumway (1982). Magnitude:Yield for nuclear explosions in granite at the Nevada Test Site and Algeria: joint determination with station effects and with data containing clipped and low-amplitude signals, *Report VSC-TR-82-12*, Teledyne Geotech, Alexandria, Virginia.
- Blandford, R. R., R. H. Shumway, R. Wagner, and K. L. McLaughlin (1983). Magnitude yield for nuclear explosions at several test sites with allowance for effects of truncated data, amplitude correlation between events within test sites, absorption, and pP, *Report TGAL-TR-83-06*, Teledyne Geotech, Alexandria, Virginia.
- Chan, W. W., K. L. McLaughlin, R.-S. Jih, M. E. Marshall, and R. A. Wager (1988). Comprehensive magnitude yield estimation for nuclear explosions: a maximum likelihood general linear model (MLE-GLM88), *Report TGAL-87-05*, Teledyne Geotech, Alexandria, Virginia.
- Chinnery, M. A. (1978). Measurements of m_b with a global network, *Tectonophysics*, 49, 139-144.
- Christoffersson, A. and F. Ringdal (1981). Optimum approaches to magnitude measurements, in *Identification of Seismic Sources - Earthquakes or Underground Explosions*, E. S.

- Husebye and S. Mykkeltveit, Editors, D. Reidel Publishing Co., Dordrecht, Holland.
- Clark, R. A. (1983). Effects of network-average magnitude bias on yield estimates for underground nuclear explosions, *Geophys. J.*, 75, 545-553.
- Dempster, A. P., N. M. Laird, and D. B. Rubin (1977). Maximum likelihood estimation from incomplete data via the EM algorithm, *J. Roy. Statist. Soc. B.* 39, 1-38.
- Douglas, A. (1966). A special purpose least squares programme, *AWRE Report No. O-54/66*, HMSO London, UK.
- Efron, B. (1979). Bootstrap methods: Another look at the jackknife, *Ann. Statist.*, 7, 1-26.
- Efron, B. (1981). Censored data and the bootstrap, *J. Am. Statist. Assoc.*, 76, 312-319.
- Efron, B. and R. Tibshirani (1985). The bootstrap method for assessing statistical accuracy, *Behaviormetrika*, 17, 1-35.
- Everndon, J. F. and W. M. Kohler (1976). Bias in estimates of m_b at small magnitudes, *Bull. Seism. Soc. Am.*, 66, 789-802.
- Gleit, A. (1985). Estimation for small normal data sets with detection limits, *Env. Sci. Tech.*, 19, 1206-1213.
- Lilwall, R. C. (1986). Some simulation studies on seismic magnitude estimations, *AWRE Report No. O-22/86*, HMSO London, UK.
- Lilwall, R. C., P. D. Marshall, and D. W. Rivers (1988). Body wave magnitudes of some underground nuclear explosions at the Nevada (USA) and Shagan River (USSR) Test Sites, *AWE Report No. O-15/88*, HMSO London, UK.

- McLaughlin, K. L. (1988). Maximum likelihood event magnitude estimation with bootstrapping for uncertainty estimation, *Bull. Seism. Soc. Am.*, 78, 855-862.
- McLaughlin, K. L., R. H. Shumway, R. O. Ahner, M. E. Marshall, T. W. McElfresh, and R. A. Wagner (1986a). Determination of event magnitudes with correlated data and censoring: a maximum likelihood approach, *Report TGAL-86-01*, Teledyne Geotech, Alexandria, Virginia.
- McLaughlin, K. L., R. O. Ahner, M. E. Marshall (1986b). Maximum likelihood event magnitudes and $\log(\max/a)$ at the Novaya Zemlya and Degelen test sites, *Report TGAL-86-02*, Teledyne Geotech, Alexandria, Virginia.
- Ringdal, F. (1976). Maximum likelihood estimation of seismic magnitude, *Bull. Seism. Soc. Am.*, 66, 789-802.
- Ringdal, F. (1986). Study of magnitudes, seismicity, and earthquake detectability using a global network, *Bull. Seism. Soc. Am.*, 76, 1641-1659.
- Schmee, J. and G. J. Hahn (1979). A simple method for regression analysis with censored data, *Technometrics*, 21, 417-432.
- Shumway, R. H. (1982). An approach to time series smoothing and forecasting using the EM algorithm, *Journal of Time Series Analysis*, 3, 253-264.
- Shumway, R. H. and A. S. Azari (1988). Estimating mean concentrations when some data are below the detection limit, *Final Report Contract ARB-A733-045*, Research Division, California Air Resources Board, California.
- Veith, K. F. and G. E. Clawson (1972). Magnitude from short-period P-wave data, *Bull. Seism. Soc. Am.*, 62, 435-452.

von Seggern, D. H. (1973), Joint magnitude determination and analysis of variance for explosion magnitude estimates, *Bull. Seism. Soc. Am.*, 63, 827-845.

von Seggern, D. and D. W. Rivers (1978). Comments on the use of truncated distribution theory for improved magnitude estimation, *Bull. Seism. Soc. Am.*, 68, 1543-1546.

(THIS PAGE INTENTIONALLY LEFT BLANK)

DISTRIBUTION LIST
FOR UNCLASSIFIED REPORTS
DARPA-FUNDED PROJECTS
(Last Revised: 26 October 1988)

<u>RECIPIENT</u>	<u>NO. OF COPIES</u>
DEPARTMENT OF DEFENSE	
DARPA/GSD ATTN: Dr. R. Alewine and Dr. R. Blandford 1400 Wilson Boulevard Arlington, VA 22209-2308	2
DARPA/PM 1400 Wilson Boulevard Arlington, VA 22209-2308	1
Defense Intelligence Agency Directorate for Scientific and Technical Intelligence Washington, D.C. 20301	1
Defense Nuclear Agency Shock Physics Washington, D.C. 20305-1000	1
Defense Technical Information Center Cameron Station Alexandria, VA 22314	2
DEPARTMENT OF THE AIR FORCE	
AFGL/LWH ATTN: Dr. J. Cipar and Mr. J. Lewkowicz Terrestrial Sciences Division Hanscom AFB, MA 01731-5000	2

AFOSR/NPG
ATTN: Director
Bldg. 410, Room C222
Bolling AFB, Washington, D.C. 20332

1

AFTAC/DA
ATTN: STINFO Officer
Patrick AFB, FL 32925-6001

1

AFTAC/TT
Patrick AFB, FL 32925-6001

3

AFWL/NTESG
Kirtland AFB, NM 87171-6008

1

DEPARTMENT OF THE NAVY

NORDA
ATTN: Technical Library
Code 543
NSTL Station, MS 39529

1

DEPARTMENT OF ENERGY

Department of Energy
ATTN: Mr. Max A. Koontz (DP-52)
International Security Affairs
1000 Independence Avenue
Washington, D.C. 20545

1

Lawrence Livermore National Laboratory
ATTN: Dr. J. Hannon and Dr. M. Nordyke
University of California
P.O. Box 808
Livermore, CA 94550

2

Los Alamos Scientific Laboratory 2
ATTN: Dr. K. Olsen and Dr. T. Weaver
P.O. Box 1663
Los Alamos, NM 87544

Sandia Laboratories 1
ATTN: Mr. P. Stokes
Geosciences Department 1255
Albuquerque, NM 87185

OTHER GOVERNMENT AGENCIES

Central Intelligence Agency 1
ATTN: Dr. L. Turnbull
OSI/NED, Room 5G48
Washington, D.C. 20505

U.S. Arms Control and Disarmament Agency 1
ATTN: Dr. M. Eimer
Verification and Intelligence Bureau, Rm 4953
Washington, D.C. 20451

U.S. Arms Control and Disarmament Agency 1
ATTN: Mr. Alfred Lieberman
VI-OA, Rm 5726
State Department Building
320 - 21st Street, NW
Washington, DC 20451

U.S. Arms Control and Disarmament Agency 1
ATTN: Mrs. M. Hoinkes
Multilateral Affairs Bureau, Rm 5499
Washington, D.C. 20451

U.S. Geological Survey 1
ATTN: Dr. T. Hanks
National Earthquake Research Center
345 Middlefield Road
Menlo Park, CA 94025

U.S. Geological Survey 1
ATTN: Dr. R. Masse
Global Seismology Branch
Box 25046, Stop 967
Denver Federal Center
Denver, CO 80225

UNIVERSITIES

Boston College 1
ATTN: Dr. A. Kafka
Western Observatory
381 Concord Road
Weston, MA 02193

California Institute of Technology 1
ATTN: Dr. D. Harkrider
Seismological Laboratory
Pasadena, CA 91125

Columbia University 1
ATTN: Dr. L. Sykes
Lamont-Doherty Geological Observatory
Palisades, NY 10964

Cornell University 1
ATTN: Dr. M. Barazangi
INSTOC
Snee Hall
Ithaca, NY 14853

Harvard University 1
ATTN: Dr. J. Woodhouse
Hoffman Laboratory
20 Oxford Street
Cambridge, MA 02138

Massachusetts Institute of Technology 3
ATTN: Dr. S. Soloman, Dr. N. Toksoz, and Dr. T. Jordan
Department of Earth and Planetary Sciences
Cambridge, MA 02139

Southern Methodist University 1
ATTN: Dr. E. Herrin
Geophysical Laboratory
Dallas, TX 75275

State University of New York at Binghamton 1
ATTN: Dr. F. Wu
Department of Geological Sciences
Vestal, NY 13901

St. Louis University 2
ATTN: Dr. O. Nuttli and Dr. R. Herrmann
Department of Earth and Atmospheric Sciences
3507 Laclede
St. Louis, MO 63156

The Pennsylvania State University 1
ATTN: Dr. S. Alexander
Geosciences Department
403 Deike Building
University Park, PA 16802

University of Arizona 1
ATTN: Dr. T. Wallace
Department of Geosciences
Tucson, AZ 85721

University of California, Berkeley 1
ATTN: Dr. T. McEvilly
Department of Geology and Geophysics
Berkeley, CA 94720

University of California Los Angeles 1
ATTN: Dr. L. Knopoff
Department of Earth and Space Sciences
3806 Geology
Los Angeles, CA 90024

University of California, San Diego 1
ATTN: Dr. J. Orcutt
Scripps Institute of Oceanography
La Jolla, CA 92093

University of Colorado
ATTN: Dr. C. Archambeau
CIRES
Boulder, CO 80309

1

University of Illinois
ATTN: Dr. S. Grand
Department of Geology
1301 West Green Street
Urbana, IL 61801

1

University of Michigan
ATTN: Dr. T. Lay
Department of Geological Sciences
Ann Arbor, MI 48109-1063

1

University of Nevada
ATTN: Dr. K. Priestley
Mackay School of Mines
Reno, NV 89557

1

University of Southern California
ATTN: Dr. K. Aki
Center for Earth Sciences
University Park
Los Angeles, CA 90089-0741

1

DEPARTMENT OF DEFENSE CONTRACTORS

Applied Theory, Inc.
ATTN: Dr. J. Trulio
930 South La Brea Avenue
suite 2
Los Angeles, CA 90036

1

Center for Seismic Studies
ATTN: Dr. C. Romney and Mr. R. Perez
1300 N. 17th Street, Suite 1450
Arlington, VA 22209

2

ENSCO, Inc. 1
ATTN: Mr. G. Young
5400 Port Royal Road
Springfield, VA 22151

ENSCO, Inc. 1
ATTN: Dr. R. Kemerait
445 Pineda Court
Melbourne, FL 32940

Gould Inc. 1
ATTN: Mr. R. J. Woodard
Chesapeake Instrument Division
6711 Baymeado Drive
Glen Burnie, MD 21061

Pacific Northwest Laboratories 1
ATTN: Dr. Wes L. Nicholson
Battelle Memorial Institute
P. O. Box 999
Richland, WA 99352

Pacific Sierra Research Corp. 1
ATTN: Mr. F. Thomas
12340 Santa Monica Boulevard
Los Angeles, CA 90025

Rockwell International 1
ATTN: B. Tittmann
1049 Camino Dos Rios
Thousand Oaks, CA 91360

Rondout Associates, Inc. 1
ATTN: Dr. P. Pomeroy
P.O. Box 224
Stone Ridge, NY 12484

Science Applications, Inc. 1
ATTN: Dr. T. Bache, Jr.
P.O.Box 2351
La Jolla, CA 92038

Science Horizons 2
ATTN: Dr. T. Cherry and Dr. J. Minster
710 Encinitas Blvd.
Suite 101
Encinitas, CA 92024

Sierra Geophysics, Inc. 2
ATTN: Dr. R. Hart and Dr. G. Mellman
11255 Kirkland Way
Kirkland, WA 98124

SRI International 1
ATTN: Dr. A. Florence
333 Ravensworth Avenue
Menlo Park, CA 94025

S-Cubed, A Division of 1
Maxwell Laboratories Inc.
ATTN: Dr. S. Day
P.O. Box 1620
La Jolla, CA 92038-1620

S-Cubed, A Division of 1
Maxwell Laboratories Inc.
ATTN: Mr. J. Murphy
11800 Sunrise Valley Drive
Suite 1212
Reston, VA 22091

Teledyne Geotech 2
ATTN: Dr. Z. Der and Mr. W. Rivers
314 Montgomery Street
Alexandria, VA 22314

Woodward-Clyde Consultants 2
ATTN: Dr. L. Burdick and Dr. J. Barker
556 El Dorado St.
Pasadena, CA 91105

NON-U.S. RECIPIENTS

National Defense Research Institute FOA 290 1
ATTN: Dr. O. Dahlman
Box 27322
S-10254 Stockholm, Sweden

Blacknest Seismological Center 1
ATTN: Mr. P. Marshall
Atomic Weapons Research Establishment
UK Ministry of Defence
Brimpton, Reading, Berks. RG7-4RS
United Kingdom

NTNF NORSAR 1
ATTN: Dr. F. Ringdal
P.O. Box 51
N-2007 Kjeller
Norway

OTHER DISTRIBUTION

To be determined by the project office 9